UC Davis
UC Davis Previously Published Works

Title

Xenosiderophore Utilization Promotes Bacteroides thetaiotaomicron Resilience during Colitis

Permalink

Journal

ISSN

Authors

Zhu, Wenhan
Winter, Maria G
Spiga, Luisella
et al.

Publication Date

DOI

Xenosiderophore utilization promotes *Bacteroides thetaiotaomicron* resilience during colitis

Wenhan Zhu[1], Maria G. Winter[1], Luisella Spiga[1], Elizabeth R. Hughes[1], Rachael Chanin[1], Aditi Mulgaonkar[2], Jenelle Pennington[2], Michelle Maas[1], Cassie L. Behrendt[3], Jiwoong Kim[4], Xiankai Sun[2], Daniel P. Beiting[5], Lora V. Hooper[3,6], Sebastian E. Winter[1,*]

[1]Department of Microbiology, UT Southwestern Medical Center, Dallas, TX 75390, USA

[2]Radiology and Advanced Imaging Research Center, UT Southwestern Medical Center, Dallas, TX 75390, USA

[3]Department of Immunology, UT Southwestern Medical Center, Dallas, TX 75390, USA

[4]Department of Population and Data Sciences, UT Southwestern Medical Center, Dallas, TX 75390, USA

[5]Department of Pathobiology, School of Veterinary Medicine, University of Pennsylvania, Philadelphia, PA 19104, USA

[6]Howard Hughes Medical Institute, UT Southwestern Medical Center, Dallas, TX 75390, USA

SUMMARY

During short-lived perturbations, such as inflammation, the gut microbiota exhibits resilience and reverts to its original configuration. Although microbial access to the micronutrient iron is decreased during colitis, pathogens can scavenge iron using siderophores. How commensal bacteria acquire iron during gut inflammation is incompletely understood. Curiously, the human commensal *Bacteroides thetaiotaomicron* does not produce siderophores, but grows under iron-limiting conditions using enterobacterial siderophores. Using RNAseq, we here identify *B. thetaiotaomicron* genes that were upregulated during *Salmonella*-induced gut inflammation and were predicted to be involved in iron uptake. Mutants in the *xusABC* locus (BT2063-2065) were defective for xenosiderophore-mediated iron uptake *in vitro*. In the normal mouse gut, the XusABC system was dispensable, while a *xusA* mutant colonized poorly during colitis. This work identifies xenosiderophore utilization as a critical mechanism for *B. thetaiotaomicron* to sustain

DECLARATION OF INTEREST

colonization during inflammation and suggests a mechanism of how interphylum iron metabolism contributes to gut microbiota resilience.

eTOC blurb:

During inflammation, the mammalian body restricts microbial access to iron. Pathogens scavenge iron using siderophores; however, how commensal bacteria acquire iron during gut inflammation is incompletely understood. Zhu *et al.* report that commensal *Bacteroides thetaiotaomicron* survives iron restriction during colitis by utilizing siderophores produced by members of the Enterobacteriaceae family.

Keywords

Gut inflammation; iron metabolism; siderophore; gut microbiota resilience; Bacteroidetes

INTRODUCTION

Communities of organisms, such as gut-associated microbial communities, often exist in a stable equilibrium with minor fluctuations. Disturbances lead to transient changes in the systems' function and composition, and the community may in time revert to the original equilibrium as the perturbation passes. Alternatively, the community may adopt a new equilibrium with properties similar to the original state. In both cases, communities exhibit a type of resilience (reviewed in (Gunderson, 2000; Lozupone et al., 2012; Sommer et al., 2017)). A timely return to the original state is referred to as engineering resilience. In contrast, the term ecological resilience refers to the amount of insult that can be tolerated before a system changes to an altered state.

Several extrinsic and intrinsic factors impact the mammalian gut microbiota. Changes in host diet and ingestion of drugs, in particular antimicrobial therapy, impact the diversity, composition, and function of gut microbial communities (reviewed in (Sommer et al., 2017; Spanogiannopoulos and Turnbaugh, 2018; Winter and Baumler, 2014)). Alterations in gut microbiota composition have been reported in human diseases, including inflammatory bowel disease, diabetes, and colorectal cancer (reviewed in (Pham and Lawley, 2014; Tamboli et al., 2004; Winter and Baumler, 2014)). Disease-associated states of the microbiota, frequently referred to as dysbiosis, exhibit permanent decreased species diversity.

Inflammation-associated dysbiosis of the gut microbiota is not merely a bystander effect, but negatively influences health of its host. Decreased diversity has been linked to decreased microbiota resilience against pathogens (Lupp et al., 2007; Stecher et al., 2007). In murine models, non-infectious colitis is communicable via the transfer of a dysbiotic microbiota into genetically susceptible hosts (Arthur et al., 2012; Garrett et al., 2010). Transfer of fecal microbiota from colorectal cancer patients into mice enhanced intestinal tumor formation (Wong et al., 2017). Targeted manipulation of the dysbiotic microbiota improved acute colitis and colitis-associated colorectal cancer (Zhu et al., 2019a; Zhu et al., 2018). Despite the importance of both engineering resilience and ecological resilience of the gut microbiota,

our understanding of the molecular mechanisms that underlie microbiota resilience is limited.

Recent studies have revealed mechanisms of how gut bacteria respond to perturbations of their niches. During intestinal inflammatory episodes, the production of antimicrobial peptides is significantly increased as an effort to restrict the bloom of harmful organisms in the gut (Muniz et al., 2012). These peptides non-specifically target conserved molecular patterns in both pathogenic and commensal bacteria, raising the question of how the commensal community could remain stable for years (Faith et al., 2013). One of the mechanisms that allow members of the phylum Bacteroidetes to be resilient to host inflammation is that these bacteria modify their lipopolysaccharide (LPS), resulting in increased resistance to antimicrobial peptides (Cullen et al., 2015). In another example, changes in the host's diet forces gut bacteria to adapt their carbon and energy metabolism (Desai et al., 2016). Gut microbes rely on dietary glycans provide essential substrates for growth, and consumption of a Western diet leads to a depletion of dietary glycans in the intestinal tract. The microbial community adapts to such changes by switching from dietary glycan degradation to foraging host-secreted mucus glycoproteins as nutrients (Desai et al., 2016).

Here, we utilized transcriptomic profiling to probe how a member of the Bacteroidetes phylum maintains fitness during enteric pathogen infection. We show that siderophore cross-feeding between different phyla of bacteria allows gut commensals to acquire iron in the inflamed gut. Our findings implicate iron metabolism as an important factor of gut microbiota resilience.

RESULTS

B. thetaiotaomicron genes related to iron metabolism are upregulated in response to infection with a pro-inflammatory pathogen.

To identify factors mediating commensal resilience in the inflamed intestine, we performed a transcriptome analysis of a defined minimal community upon challenge with a pro-inflammatory enteric pathogen, *Salmonella enterica* serovar Typhimurium (*S*. Tm). *S*. Tm is a common cause of bacterial foodborne gastroenteritis. In mice, experimental infection results in subacute intestinal inflammation. Groups of gnotobiotic mice were associated with two human isolates, *B. thetaiotaomicron* and *Clostridium symbiosum*, representing the predominant phyla in the human gut microbiota (Bacteroidetes and Firmicutes). After 7 days, we infected one group with the *S*. Tm wild-type strain while the mock treatment group received sterile LB broth. Two days later, we extracted total RNA from cecal contents and determined the transcriptome by high-throughput RNA sequencing (RNAseq) (Fig. 1A). We generated a *Bacteroides*-specific transcriptome by mapping unambiguous reads to the genome of *B. thetaiotaomicron* VPI-5482. *S*. Tm infection profoundly altered the gene expression profile of *B. thetaiotaomicron* in the murine cecum (Fig. 1B), with 364 genes being differentially transcribed in response to *S*. Tm infection (Fig. 1C; Table S1). The predicted primary amino acid sequence of several of these genes shared limited sequence similarity with proteins involved in iron uptake in other bacteria. This finding suggests that, as essential micronutrients including iron become limited during gut inflammation (Deriu et

al., 2013; Raffatellu et al., 2009), *B. thetaiotaomicron* adapts its iron metabolism to optimize fitness during *S*. Tm infection. While bacterial pathogens employ a plethora of strategies to overcome nutritional immunity (Caza and Kronstad, 2013), our understanding of how commensal gut bacteria acquire iron during gut inflammation is incomplete. We thus focused on investigating iron metabolism in *B. thetaiotaomicron.*

Bacteroides strains isolated from the murine gut utilize enterobacterial siderophores *in vitro*

We first investigated iron uptake of *B. thetaiotaomicron* under laboratory conditions. One strategy used by bacterial pathogens to overcome iron limitation imposed by the host immune responses is to produce low molecular weight, high-affinity iron chelators termed siderophores. *B. thetaiotaomicron* utilizes heme iron for growth *in vitro*, but does not produce any known siderophores (Manfredi et al., 2015; Rocha et al., 1991; Verweijvanvught et al., 1988). Consequently, *B. thetaiotaomicron* grows poorly in TYG media supplemented with 200 μM of the metal chelating agent bathophenanthroline disulfonate (BPS) (Fig. 2A). BPS acts as a buffer to chelate free iron and addition of small amounts of iron salts (10 μM) does not restore growth (Fig. S1A). This growth defect is rescued by addition of 200 μM ammonium iron citrate, indicating that the inability to access iron, and not other trace metals, was responsible for diminished growth (Fig. S1B). In contrast, *S*. Tm produces two catecholate siderophores, enterobactin and salmochelin, and grows under iron-limiting, anaerobic conditions *in vitro* (Hantke et al., 2003; Muller et al., 2009; Pollack and Neilands, 1970)(Fig. 2A). Some bacterial species do not produce siderophores but instead utilize siderophores that are produced by other microbes, a phenomenon sometimes referred to as xenosiderophore utilization or siderophore piracy. We thus tested a small panel of enterobacterial siderophores for their ability to enhance growth of *B. thetaiotaomicron* in BPS-supplemented media. Consistent with a previous report (Rocha and Krykunivsky, 2017), growth in BPS-supplemented media was restored by the addition of purified, iron-laden enterobactin or salmochelin (Fig. 2B; Fig. S1C), suggesting that *B. thetaiotaomicron* may acquire iron through xenosiderophore uptake.

To study xenosiderophore-mediated iron uptake in a more controlled setting, we depleted trace elements from media using a polyvalent ion exchange resin, added back trace elements except iron, and assessed growth of *B. thetaiotaomicron* (Fig. S2A). The apo form of both catecholate siderophores was unable to support growth of the *B. thetaiotaomicron* wild-type, while supplementation with ferric-enterobactin or ferric-salmochelin markedly increased growth (Fig. S2A). We performed analogous experiments with *S*. Tm mutants defective for catecholate siderophore production (*entB* mutant) and uptake (*fepA iroN cirA* mutant) as controls (Baumler et al., 1998; Klebba et al., 1982; Rabsch et al., 2003; Rabsch et al., 1999; Wookey and Rosenberg, 1978)(Fig. S2B). These experiments provide further evidence that *B. thetaiotaomicron* can overcome iron limitation by using xenosiderophores.

We then explored whether xenosiderophore utilization is a phenomenon specific to *B. thetaiotaomicron*. We isolated several *Bacteroides* species from our mouse vivarium and tested whether they utilize enterobactin or salmochelin during anaerobic growth *in vitro* (Fig. 2C). Addition of iron-laden enterobactin or salmochelin enhanced growth of murine

Bacteroides vulgatus and other Bacteroides species in BPS-supplemented media. As such, *Bacteroides* exhibit varying capacities to utilize catecholate xenosiderophores to support growth under iron-limiting conditions.

The *xusABC* genes are required xenosiderophore uptake *in vitro*.

We next sought to determine the genetic requirements for *B. thetaiotaomicron* to utilize enterobactin. Siderophore uptake in Gram-negative bacteria typically involves an outer membrane TonB-dependent receptor which transports iron-laden siderophores into the periplasmic space. In the periplasmic space, a siderophore binding protein relays the siderophore onto an ABC-transporter which transports the siderophore into the cytoplasm (Frost and Rosenberg, 1975; Pugsley and Reeves, 1976; Skare et al., 1993; Wookey and Rosenberg, 1978). In our transcriptome analysis, we identified several genes whose products might be involved in iron uptake or were predicted to be TonB-dependent receptors of unknown function. We generated a small library of clean deletion mutants in candidate genes and determined their fitness under iron-limiting conditions in comparison to the wild-type strain (Fig. S3). To quantify abundance, individual strains were marked with signature tags in a neutral locus in their genome (Goodman et al., 2009; Martens et al., 2008). In the presence of iron-laden enterobactin or salmochelin, the wild-type strain outgrew a mutant lacking the BT2063-2065 locus. Given its role in xenosiderophore utilization (Fig. S3), we renamed the genes in this locus *xusABC* (xenosiderophore utilization system; Fig. 3A).

We next created clean, in-frame deletion mutants in *xusA* (BT2065)*, xusB* (BT2064), and *xusC* (BT2063); the *xusA* strain was complemented by introducing the *xusA* gene under control of its native promoter in the BT3743-3744 intergenic region, a neutral locus in the *B. thetaiotaomicron* chromosome (Lim et al., 2017). The *xusA* mutant did not display any growth defects in rich media (Fig. S3B), indicating that the *xusA* mutant is not defective in general iron metabolism. Under iron-limiting conditions, growth of the wild-type and the mutant strains was impeded (Fig. 3B). Importantly, supplementation with purified, iron-laden enterobactin or salmochelin rescued the growth defect of the wild-type strain while the *xusA, xusB*, and *xusC* mutants did not benefit from siderophore supplementation (Fig. 3B; Fig. S1B **and** S2A). Genetic complementation of *xusA* restored the ability to grow in the presence of siderophores (Fig. 3B). Furthermore, supplementation with excess iron citrate reversed the growth defect of the *xusA* mutant in BPS-supplemented media (Fig. S1B **and** S2A).

The *xusA* gene is predicted to encode a putative TonB-dependent receptor. To monitor iron acquisition more directly, we cultured *B. thetaiotaomicron* in iron-deprived media to exhaust endogenous iron before we supplemented the culture with either vehicle or iron-laden enterobactin. We then employed Inductively Coupled Plasma Mass Spectrometry (ICP-MS) to assess cellular iron levels (Fig. 3C). Supplementation of the growth media with iron-laden enterobactin significantly increased the cellular iron levels of the wild-type strain compared to the iron-depleted growth condition. In contrast, cellular iron levels in the *xusA* mutant were unaffected by enterobactin availability in the growth media (Fig. 3C), suggesting that XusA is required for enterobactin-mediated iron uptake.

The *B. thetaiotaomicron xusABC* locus is required for colonization during murine *S.* Tm infection.

Next, we investigated the availability of iron in the intestinal contents during *Salmonella* infection. We intragastrically inoculated streptomycin-pretreated C57BL/6 mice with *S.* Tm or LB broth. After 4 days, we quantitated chelatable and total iron levels in the cecal contents by ICP-MS. Both iron pools decreased substantially during *S.* Tm infection when compared to mock-treated animals (Fig. 4A), suggesting that iron indeed becomes limited during *S.* Tm infection.

S. Tm relies on catecholate siderophores to overcome iron limitation during infection. Mutants unable to produce or utilize enterobactin or salmochelin are attenuated in mouse models of infection (Costa et al., 2016; Deriu et al., 2013; Diaz-Ochoa et al., 2016; Karlinsey et al., 2019; Nagy et al., 2013; Nagy et al., 2014; Raffatellu et al., 2009). To detect siderophore production in the murine intestinal contents, we developed a simple assay that relies on growth of a bacterial reporter strain *in vitro*. The isochorismatase EntB catalyzes the conversion of isochorismate to 2,3-dihydroxy-2,3-dihydrobenzoate, a precursor for 2,3-dihydroxybenzoic acid as well as the subsequent biosynthesis of enterobactin and salmochelin (Hantke et al., 2003). As such, *entB* mutants in Enterobacteriaceae are defective to produce these siderophores (Luke and Gibson, 1971; Young et al., 1971). In BPS-containing media, growth of a *S.* Tm *entB* mutant depends on exogenous supplementation with siderophores in a dose-dependent manner (Fig. S4A). We colonized two groups of gnotobiotic mice with *B. thetaiotaomicron* and infected one group with the *S.* Tm wild-type strain and one group with a mutant unable to produce catecholate siderophores (*entB* mutant)(Fig. S4B). We then incubated filter-sterilized homogenates of the intestinal contents of these mice with the reporter strain and monitored growth (Fig. S4). Only the homogenates obtained from mice infected with the *S.* Tm wild-type strain supported robust growth of the reporter strain, consistent with the idea that *S.* Tm produces siderophores when colonizing the murine large intestine.

We then explored whether xenosiderophore utilization is required for *B. thetaiotaomicron* to colonize the mammalian intestinal tract. As *B. thetaiotaomicron* does not readily colonize conventionally-raised mice (Lee et al., 2013), we pretreated C57BL/6 mice with a cocktail of antibiotics to facilitate engraftment of *B. thetaiotaomicron* (Curtis et al., 2014) (Fig. 4B). We colonized antibiotic-treated mice with an equal mixture of the *B. thetaiotaomicron* wild-type strain and a *xusA* mutant (marked with unique signature tags; competitive colonization assay). After two days, animals were intragastrically infected with the *S.* Tm wild-type strain or mock-treated with LB broth. The abundance of each *B. thetaiotaomicron* strain in the cecal contents was determined four days post infection by qPCR using primers specific for genome-integrated signature tags. In mock-treated animals, the wild-type *B. thetaiotaomicron* strain and the *xusA* mutant displayed similar levels of fitness (Fig. 4C). In contrast, the *B. thetaiotaomicron* wild-type strain outcompeted the *xusA* mutant by more than 3 orders of magnitude in mice infected with *S.* Tm. These results suggest that *xus*-mediated iron uptake is necessary for optimal fitness of *B. thetaiotaomicron* during pathogen-induced colitis.

To more directly test the idea that xenosiderophore utilization contributes to gut colonization during colitis, we colonized two groups of antibiotic-treated mice with either the *B. thetaiotaomicron* wild-type strain, a ∆*xusA* mutant, or the complemented *xusA* mutant (∆*xusA xusA*+) (Fig. 4D–F). After two days, half of the animals in each group were euthanized to assess the colonization levels of these strains at homeostatic conditions. The remaining animals were infected with *S*. Tm. Four days after infection, we determined the abundance of *B. thetaiotaomicron* and *S*. Tm by plating on selective media. Under steady state conditions, the *B. thetaiotaomicron* wild-type strain, the ∆*xusA* mutant, and the complemented strain (∆*xusA xusA*+) were recovered at similar levels (Fig. 4E), consistent with our previous finding that the *xusA* gene is dispensable for fitness under homeostatic conditions (Fig. 4C). In contrast, the *B. thetaiotaomicron* ∆*xusA* mutant colonized the cecum of *S*. Tm-infected mice at significantly lower levels than the *B. thetaiotaomicron* wild-type strain (Fig. 4E). The colonization defect observed for the ∆*xusA* mutant upon *S*. Tm infection was fully restored in the complemented strain. No significant differences in *S*. Tm gut colonization or markers of mucosal inflammation were noted (Fig. 4F; Fig. S5A). Similar results were obtained when the experiment was performed with *B. thetaiotaomicron* strains carrying genome-integrated signature tags (Fig. S5B–E).

Furthermore, we determined whether transcription of *xusABC* genes was induced as a result of *S*. Tm infection (Fig. S6). Mice pre-colonized with *B. thetaiotaomicron* were infected with *S*. Tm or mock-treated and RNA extracted from the colon content. mRNA levels of *xusA*, *xusB*, and *xusC*, normalized to the housekeeping gene *gmk*, were determined by RT-qPCR. Transcription of all three genes was markedly induced in *S*. Tm-infected animals (Fig. S6B). In this model, populations of other gut commensals are present (Fig. S6C–E), thus validating our initial transcriptomic analysis in gnotobiotic animals (Fig. 1). Collectively, these data suggest that utilization of xenosiderophores through the XusABC system is important for *B. thetaiotaomicron* to maintain efficient gut colonization in the setting of enteric pathogen infection.

Enterobacterial siderophores contribute to *B. thetaiotaomicron* fitness during S. Tm infection.

We next examined the origin of the siderophores used by the *B. thetaiotaomicron* XusABC system. *S*. Tm produces both enterobactin and salmochelin. As such, we predicted that the fitness defect of a *B. thetaiotaomicron xusA* mutant would be rescued when mice are infected by a *S*. Tm mutant unable to produce siderophores (*S*. Tm ∆*entB* mutant) (Fig. 5A–C). As expected, the *B. thetaiotaomicron* ∆*xusA* mutant colonized the colon of *S*. Tm-infected mice at significantly lower levels than the wild-type strain (~360-fold fitness defect; Fig. 5B). In contrast, the fitness defect mice infected with the *S*. Tm ∆*entB* mutant was drastically reduced (8.7-fold fitness defect; Fig. 5B). This experiment suggests that during *S*. Tm infection, the siderophore pool accessed by *B. thetaiotaomicron* is primarily derived from *S*. Tm siderophores, with a minor contribution of siderophores from other members of the gut microbiota.

Commensal Enterobacteriaceae family members produce siderophores that could be utilized by *B. thetaiotaomicron* for iron acquisition. *E. coli* is considered a member of the "core

microbiota" shared by the majority of humans and *E. coli* strains are frequently isolated from human feces (Lozupone et al., 2012; Mitsuoka and Hayakawa, 1973; Penders et al., 2006). For example, *E. coli* Nissle 1917 strain produces and utilizes four distinct siderophores: enterobactin, salmochelin, yersiniabactin, and aerobactin and thus represents a useful tool for investigating iron metabolism in Enterobacteriaceae (Deriu et al., 2013). We hypothesized that siderophores produced by commensal *E. coli* could contribute to the siderophore pool utilized by commensal *B. thetaiotaomicron* during inflammatory conditions. To test this idea, we colonized antibiotic-treated mice with an equal mixture of *B. thetaiotaomicron* wild-type and the *xusA* mutant as described above (competitive colonization assay) (Fig. 5D). Mice were then intragastrically inoculated with a Nissle 1917 *entB* mutant as well as a *S.* Tm *entB* mutant (group 1). Because defects in siderophore production attenuates *S.* Tm virulence and gut colonization (Crouch et al., 2008; Raffatellu et al., 2009; Sassone-Corsi et al., 2016)(Fig. 5C), we used lipocalin-2-deficient (*Lcn2*) mice on the C57BL/6 background. Lipocalin-2, a protein released by neutrophils and epithelial cells, sequesters enterobactin, thus impeding bacterial iron acquisition through enterobactin. In Lcn2-deficient mice, the *S.* Tm *entB* mutant and the Nissle 1917 *entB* mutant efficiently colonized the large intestine (Fig. 5E and F). The *B. thetaiotaomicron* wild-type and the *xusA* mutant were present in the colonic contents at low, but similar levels (Fig. 5G). This outcome suggests that in the absence of enterobacterial siderophore production, *B. thetaiotaomicron* was unable to benefit from siderophore utilization by the XusABC system. We then repeated this experiment and colonized groups of mice with either the Nissle 1917 wild-type strain and a *S.* Tm *entB* mutant (group 2) or a Nissle 1917 *entB* mutant and the *S.* Tm wild-type strain (group 3) (Fig. 5D). We observed no differences in Nissle 1917 and *S.* Tm populations in the colonic contents (Fig. 5E and F). In both groups (group 2 and 3), the *B. thetaiotaomicron* wild-type population colonized the colon lumen at high levels, while the *B. thetaiotaomicron* *xusA* mutant was unable to benefit from enterobacterial siderophore production (Fig. 5G). Taken together, these findings suggest that the *B. thetaiotaomicron* XusABC system only provides a fitness advantage in the context of siderophore production by Enterobacteriaceae family members.

We also explored whether siderophore production by *S.* Tm enhances fitness of other members of the genus *Bacteroides*. We colonized antibiotic treated mice with two *Bacteroides* strains (*B. vulgatus* WZ748 and *Bacteroides sp.* WZ837) that utilize catecholate siderophores under iron-limiting conditions in the laboratory (Fig. 2C). These animals were then either infected with the *S.* Tm wild-type, an isogenic *entB* mutant, or mock-treated (Fig. 6A). *Bacteroides sp.* WZ837 was recovered at a significantly higher level in mice challenged by the *S.* Tm wild-type strain than those that had received the isogenic *entB* mutant (Fig. 6B), suggesting that this strain benefited from enterobacterial siderophores. In contrast, the *B. vulgatus* isolate showed no difference in colonization levels as a result of *S.* Tm siderophore production (Fig. 6C). This outcome suggests that members of the genus Bacteroides likely utilize divers, and possibly redundant, pathways for iron acquisition.

Enterobacterial siderophores enhance *B. thetaiotaomicron* fitness in mouse models of non-infectious colitis

Lastly, we determined whether cross-feeding of siderophores commensal *E. coli* and *B. thetaiotaomicron* also occurs in a setting of non-infectious colitis. *Il10*-deficient mice spontaneously develop colitis under laboratory conditions. Administration of oral non-steroidal anti-inflammatory drugs, such as piroxicam, accelerate this process (Hale et al., 2005). We treated *Il10*-deficient C57BL/6 mice with oral antibiotics as described above. One group of animals was then intragastrically inoculated with an equal mixture of the *B. thetaiotaomicron* wild-type and the *xusA* mutant (competitive colonization assay), as well as a Nissle 1917 *entB* mutant (Fig. 7A). A second group was similarly inoculated with the two *B. thetaiotaomicron* strains as well as the Nissle 1917 wild-type strain. Both groups were treated with piroxicam throughout the entire experiment. Samples of intestinal contents were collected 14 days after colonization with *B. thetaiotaomicron* and *E. coli*, and bacterial populations were quantified by plating luminal contents on selective media (Fig. 7B and C). Both the Nissle 1917 and the isogenic *entB* mutant colonized the large intestine to similar levels (Fig. 7B). This observation is consistent with the idea that in the absence of enterobactin and salmochelin production, Nissle 1917 may rely on other siderophores such as aerobactin or yersiniabactin to acquire iron. Notably, the XusABC system only provided a fitness advantage in mice colonized by the Nissle 1917 wild-type strain (Fig. 7C). The XusABC system did not confer any fitness advantage in the absence of catecholate siderophore production by Nissle 1917 (*entB* mutant). No differences in inflammatory markers were observed in the two treatment groups (Fig. S7). This experiment demonstrates that cross-feeding of siderophores between *B. thetaiotaomicron* and commensal Enterobacteriaceae occurs in the inflamed intestinal tract.

DISCUSSION

Resilience is an important feature of the gut microbiota in the context of inflammatory diseases. *Bacteroides* species are highly abundant in the microbiota of the mammalian large intestine and fulfill many pivotal functions for human health. For instance, anaerobic fermentation of complex dietary glycans by members of the Bacteroidetes phylum results in production of large quantities of short chain fatty acids, in particular propionate (Fischbach and Sonnenburg, 2011; Martens et al., 2014). Microbiota-derived propionate modulates T cell differentiation by inhibiting histone-deacetylase activity (Arpaia et al., 2013; Luu et al., 2018). In addition, propionate produced by *B. thetaiotaomicron* has been shown to inhibit growth of *S.* Tm in a mouse model of infection (Jacobson et al., 2018; Sorbara et al., 2019). It is therefore plausible that a more resilient microbial community enables the host to recover from enterobacterial pathogen challenges with faster kinetics and less severe host inflammatory responses.

The molecular mechanisms that mediate ecological or engineering resistance in the gut microbiota are beginning to be uncovered. Previous work suggests that *Bacteroides* species respond to the release of antimicrobial peptides by modifying their surface (Cullen et al., 2015). Furthermore, during nutrient limitation caused by the lack of dietary fiber, *Bacteroides* species resort to degrading host-derived glycoproteins as nutrient sources (Desai

et al., 2016). Here, we present evidence that during inflammation-associated iron limitation, members of the Bacteroidetes phylum rely on the xenosiderophores enterobactin and salmochelin for iron acquisition. We identified a set of genes, *xusABC*, which are required for enterobactin and salmochelin utilization in *B. thetaiotaomicron* VPI-5482. XusABC-mediated xenosiderophore uptake was dispensable under homeostatic conditions, consistent with the idea that *Bacteroides* acquire iron from other sources, such as heme iron (Otto et al., 1990; Rocha et al., 1991) or transferrin (Manfredi et al., 2015), under these conditions. During colitis, microbial access to metals is limited, presumably by the release of lactoferrin and calprotectin (reviewed in (Hood and Skaar, 2012; Lopez and Skaar, 2018; Zhu et al., 2019b)). We found that the XusABC system was required for *B. thetaiotaomicron* VPI-5482 to efficiently maintain gut colonization during pathogen-induced (*S*. Tm infection) and non-infectious colitis (*Il10*/piroxicam-induced colitis).

Enterobactin and salmochelin are typically produced by Enterobacteriaceae family members. In our mouse models, the fitness advantage conferred by the XusABC system was markedly reduced when mice were colonized with *E. coli* and *S*. Tm mutants defective for enterobactin and salmochelin production (*entB* mutants; Fig. 5). This suggests that the experimentally introduced *E. coli* and *S*. Tm are a major source of enterobactin and salmochelin in our experiment. The XusABC system enhances colonization when iron accessibility is limited and siderophore-producing Enterobacteriaceae are present. The *E. coli* wild-type strain or *S*. Tm wild-type were each sufficient to permit *B. thetaiotaomicron* to benefit from xenosiderophore utilization through the XusABC system (Fig. 5). As such, both commensal and pathogenic Enterobacteriaceae can serve as the source of siderophores for *B. thetaiotaomicron*. Since *B. thetaiotaomicron* only relies on xenosiderophore utilization during specific environmental conditions that are conducive for siderophore production by Enterobacteriaceae, such as infection with an enterobacterial pathogen or non-infectious colitis (Raffatellu et al., 2009), it is tempting to speculate that may be little evolutionary pressure for *B. thetaiotaomicron* to maintain the ability to produce siderophores (Rocha et al., 1991; Verweijvanvught et al., 1988).

In vitro, the XusABC system was specific for two structurally related catecholate siderophores, enterobactin and salmochelin (Fig. 2). Salmochelin is a glucosylated derivative of enterobactin (Hantke et al., 2003). Since microbial siderophores exhibit vast structural variability (Hider and Kong, 2010), it is conceivable that other siderophores that are structurally similar to enterobactin and salmochelin could be utilized by the XusABC system. In the murine gut, enterobacterial enterobactin and salmochelin are likely to be the sole siderophores that allow *B. thetaiotaomicron* to acquire iron through the XusABC system since genetic ablation of enterobacterial enterobactin and salmochelin production rendered the XusABC system inefficacious (Fig. 5).

The XusABC system we identified is predicted to be composed of a putative TonB-dependent outer membrane transporter (XusA) and an inner membrane permease (XusC). The primary amino acid sequence of XusB may contain a signal that could lead to lipidation and export, suggesting that this protein may localize to the periplasm or possibly to the cell surface (Lauber et al., 2016; Wexler et al., 2018). Some aspects of the architecture of this system may be analogous to the FepABCDG system in *E. coli* and the FhuABCD system in

Salmonella enterica. However, there is little sequence homology shared by the *B. thetaiotaomicron* XusABC components with known siderophore transport systems. Interestingly, utilization of the xenosiderophores requires the release of iron from the siderophore upon reaching the cytoplasm. Generally, there are two distinct mechanisms of iron release from siderophores. Because siderophores display significantly higher affinity towards iron (III) than iron (II), some bacterial species employ ferric reductases to reduce siderophore-bound iron (III) to iron (II) to facilitate its dissociation. Other bacterial species such as *E. coli* hydrolyze the siderophore through the action of esterases to release iron. Based on protein homology, we did not identify any ferric reductases or siderophore esterases in *B. thetaiotaomicron*, and how this bacterium releases iron from siderophores remains to be investigated.

In addition to xenosiderophores, *Bacteroides* use TonB-dependent outer membrane receptors to acquire corrinoids produced by other members of the gut microbiota (Goodman et al., 2009). *B. thetaiotaomicron* mutants defective for several redundant corrinoid uptake systems were less fit in colonizing the murine intestinal tract (Degnan et al., 2014; Wexler et al., 2018). In contrast to corrinoid uptake, which occurs under homeostatic conditions, xenosiderophore uptake was only relevant under inflammatory conditions. These examples of competition for corrinoids and siderophores highlight the complex nutritional interactions between members of the gut microbiota as it relates to micronutrient metabolism.

Nissle 1917 is an *E. coli* strain isolated from a soldier resistant to *Shigella* infection. It is currently a probiotic strain approved in certain European countries (Sonnenborn, 2016). It is effective in maintaining remission in a subset of ulcerative colitis patients (Kruis et al., 2004; Kruis et al., 1997; Rembacken et al., 1999). The molecular mechanisms associated with these probiotic properties are incompletely understood, but may be in part attributed to its ability to produce several distinct siderophores (Deriu et al., 2013). In mouse models of *Salmonella* infection, *E. coli* Nissle 1917 competes with the luminal *Salmonella* population for metals, such as iron and zinc, thus reducing pathogen burden and shedding (Deriu et al., 2013). Our data suggest that an additional mechanism may contribute to the probiotic potential of Nissle 1917. By producing catecholate siderophores, Nissle 1917 may enhance colonization by commensal *Bacteroides* during inflammatory episodes and thus increase microbiota resilience. In turn, increased commensal colonization may assist with pathogen clearance (Endt et al., 2010).

STAR METHODS

LEAD CONTACT AND MATERIALS AVAILABILITY.

Further information and requests for resources and reagents should be directed to the Lead Contact, Sebastian E. Winter (Sebastian.Winter@UTSouthwestern.edu). All plasmids and bacterial strains generated in this study are available from the Lead Contact with a completed Materials Transfer Agreement.

EXPERIMENTAL MODEL AND SUBJECT DETAILS

Bacterial strains and growth conditions.—The bacterial strains used in this study are listed in the Key Resource Table. *E. coli* and *S.* Typhimurium strains were routinely grown in LB broth (10 g/L tryptone, 5 g/L yeast extract, 10 g/L sodium chloride) or on LB plates (LB broth, 15 g/L agar) at 37 ºC. When appropriate, antibiotics were added at the following concentrations: 100 µg/mL streptomycin (Strep), 100 µg/mL ampicillin, 50 µg/ml nalidixic acid (Nal), 100 µg/mL kanamycin (Kan), 50 µg/mL gentamycin (Gen) and 15 µg/mL chloramphenicol (Cm). *B. thetaiotaomicron* was grown anaerobically (90 % N_2, 5 % CO_2, 5 % H_2; anaerobic chamber, Sheldon Manufacturing) in hemin supplemented brain-heart-infusion (BHI) media (0.8 % brain heart infusion from solid, 0.5 % peptic digest of animal tissue, 1.6 % pancreatic digest of casein, 0.5% sodium chloride, 0.2 % glucose, 0.25 % disodium hydrogen phosphate, 0.005 % haemin, pH 7.4) or hemin-supplemented TYG media (0.5 % tryptone, 0.5 % peptone, 0.5 % bacto yeast extract, 0.2 % glucose, 0.05 % cysteine, 0.1 M potassium phosphate, 1 ng/L vitamin K, 0.8 % $CaCl_2$, 0.04 µg/L ferrous sulfate, 1 µg/L resazurin, 0.02 g/L magnesium sulfate heptahydrate, 0.4 g/L sodium bicarbonate, 0.08 g/L sodium chloride, pH = 7.2) for 24 h or on blood agar plates (37 g/L brain heart infusion, 15 g/L agar, 5 % [v/v] defibrinated blood) containing 50 µg/mL Gen or 15 µg/mL Cm for 2 days at 37 ºC. *C. symbiosum* was routinely cultured in pre-reduced thioglycollate medium (0.5 % yeast extract, 1.5 % pancreatic digest of casein, 0.5 % glucose, 0.05 % L-Cysteine, 0.25 % sodium chloride, 0.05 % sodium thioglycollate, 0.0001 % resazurin, 15 g/L agar, pH 7.1) or chopped meat broth (BD) in Hungate tubes. For *in vitro* dependence on iron-laden siderophores, single colonies of indicated strains were inoculated in hemin supplemented BHI media and grown anaerobically for 24 hours and sub-cultured (1×10^3 CFU/ml) into iron restricting media (BHI or TYG supplemented with 0.005 % protoporphyrin IX and 200 µmol/L bathophenanthroline disulfonate (BPS), pH 7.4) (Rocha and Krykunivsky, 2017) and further cultured anaerobically for 36 h. Iron-laden enterobactin and salmochelin (at 50 % saturation) were added at a final concentration of 0.5 µmol/L and 2 µmol/L, respectively. The apo-forms of these siderophores were added to media at identical concentrations. To demonstrate that the absence of iron, but not other trace elements, is responsible for the growth defect observed when BPS was supplemented, ammonium iron (III) citrate was supplemented at a concentration of 200 µmol/L.

To test whether the trace metal ions other than iron are responsible for supporting bacterial growth when BPS was supplemented, divalent ions were removed from a modified semi-defined media (1.5 g/L KH_2PO_4, 0.5 g/L NH_4SO_4, 0.9 g/L NaCl, 150 mg/L L-methionine, 5 µg/L vitamin B_{12}, 1 mg/L resazurin, 1 g/L tryptone, 0.2% $NaHCO_3$,) (Rocha and Smith, 2004) as previously described (Anderson et al., 2017; Yep et al., 2014). Briefly, the semi-defied media was mixed with 1 g/L Chelex 100 Resin (Biorad, USA) under rotary agitation at 4 °C overni ght. 1 g/L L-cysteine, 5 mg/L protoporphyrin IX, and 5 g/L glucose were added to the media and further incubated with additional Chelex 100 Resin (1 g/L) for 3 hours at 4 °C. The media was supplemented with divalent ions except iron (200 mg/L $MgCl_2$ × 6 H_2O, 100 mg/L $CaCl_2$ × 2 H_2O, 10 mg/L $MnCl_2$ × 4 H_2O, 10 mg/L $CoCl_2$ × 6 H_2O, 100 mg/L $ZnCl_2$, 10 mg/L $CuSO_4$, 10 mg/L Na_2MoO_4), and sterilized by passing through a 0.22 µm filter. Overnight cultures of *B. thetaiotaomicron* or *S.* Tm were washed twice using iron-

free semi defined media to remove cell-associated iron before inoculation. The inoculum for these experiments was 10^4 CFU/ml.

For isolating members of phylum Bacteroidetes from the murine large intestinal tract, cecal and colonic contents of wild-type C57BL/6 mice were collected in phosphate buffered saline (PBS) supplemented with 0.05% L-cysteine. The contents were then plated on Bacteroides Bile Esculin Agar (Becton Dickinson, USA) and incubated anaerobically until colonies were observed. Single colonies were further purified using Bacteroides Bile Esculin Agar and the bacterial strains were identified by sequencing the V3-V4 region of 16S rDNA and comparing the sequences to the RDP database (https://rdp.cme.msu.edu/). The isolated Bacteroidetes strains were routinely propagated in hemin supplemented brain-heart-infusion (BHI) media. Of note, both Bacteroides isolates used in this manuscript (*Bacteroides* sp. WZ837 and *Bacteroides vulgatus* WZ748) are resistant to gentamycin.

Animal models.—C57BL/6J wild-type, *Il10*$^{-/-}$, and *Lcn2*$^{-/-}$ mice, originally obtained from Jackson Laboratory (Bar Harbor), were bred under specific pathogen-free conditions at UT Southwestern Medical Center. Mice had *ad libitum* access to irradiated feed (16 % protein; Envigo) and autoclaved water, and were on a 12 h light-dark cycle. All animals were treatment naïve and healthy prior to our studies. Seven to nine-week-old male and female mice were semi-randomly assigned into treatment groups before the experiment.

Antibiotic cocktails (5 mg of each of ampicillin (Cayman Chemicals), metronidazole (Sigma), vancomycin (Chem Impex International) and neomycin (Sigma) per mouse) or mock treatment (water) were administered by oral gavage daily for 5 days. After antibiotic treatment, fecal pellets were collected and tested for bacterial growth on blood agar and blood agar supplemented with 50 μg/mL gentamycin. Only mice with no detectable bacterial growth on both media were included in the study to allow for quantification of experimentally-introduced *Bacteroides* strains in luminal content and feces. At day 5, mice were then inoculated with 3×10^9 CFU of the indicated *B. thetaiotaomicron* strains, or mouse *Bacteroides* isolates, or remained uninfected. In competitive colonization experiments, animals were inoculated with an equal mixture of 1.5×10^9 CFU of the *B. thetaiotaomicron* wild-type strain and 1.5×10^9 CFU of the indicated mutants. Two days later, mice were challenged by 1×10^9 CFU of the *S.* Typhimurium strain SL1344 for 4 days (Fig. 4 and 5A–C). For experiment involving *E. coli* Nissle 1917 and *S.* Typhimurium (**Fig. 6D-G**), animals were inoculated with an equal mixture of 1×10^9 CFU of the *B. thetaiotaomicron* wild-type strain, or 1×10^9 CFU of indicated *B. thetaiotaomicron* mutant at day 5. Two days after inoculation, mice were challenged with 1×10^9 CFU of indicated *E. coli* Nissle 1917 strain and 1×10^9 CFU of the indicated *S.* Typhimurium strain. For the non-infectious colitis model (*Il10*$^{-/-}$)(Fig. 7), animals were inoculated with an equal mixture of 1×10^9 CFU of WT *B. thetaiotaomicron* strain, 1×10^9 CFU of indicated *B. thetaiotaomicron* mutant, and 1×10^9 CFU of indicated *E. coli* strain at day 5. Piroxciam (Sigma-Aldrich) was administered in the mouse feed (Envigo) at a concentration of 100 ppm for 19 days to accelerate colitis development.

For all experiments, fecal pellets were collected at the indicated time points. After euthanasia, cecal and colonic tissue was collected, flash frozen, and stored at −80 °C for

subsequent mRNA analysis. For culture-dependent quantification of bacterial load, colonic and cecal contents were harvested in sterile PBS and the load of *B. thetaiotaomicron*, *S.* Tm, and *E. coli* were quantified by plating serial-diluted intestinal contents on selective agar. For culture-independent quantification, total DNA was extracted using QIAamp PowerFecal DNA Kit (Qiagen, CA) per manufacturer's recommendations. The samples were eluted in 100 μl elution buffer and 2 μl was used to determine the bacterial load of the *B. thetaiotaomicron* and *S.* Typhimurium strains via qPCR with primers targeting strain-specific signature tags and primers specific for Enterobacteriaceae, respectively (Martens et al., 2008; Winter et al., 2013). Relevant primers are listed in Table S2.

Gnotobiotic mouse experiments.—Germ-free Swiss-Webster mice were maintained in plastic gnotobiotic isolators on a 12-hour light cycle. Mice were randomized and orally gavaged with 3×10^9 CFU of *B. thetaiotaomicron* and 3×10^9 CFU of *C. symbiosum* strains or remained uninfected. Seven days later, mice were challenged with 1×10^5 CFU of *S.* Typhimurium strain IR715 for 2 days. After euthanasia, cecal and colonic tissue was collected in RNAlater solution (Invitrogen, USA), flash frozen and stored at −80 °C for subsequ ent mRNA analysis. Total RNA was extracted as described above.

METHOD DETAILS

Iron-laden siderophores.—The iron-free siderophores enterobactin (Sigma-Aldrich) and salmochelin S4 (Genaxxon bioscience) were dissolved in dimethyl sulfoxide (DMSO) at the concentration of 2 mmol/L. The siderophores were filter-sterilized using 0.22 μm cellulose membrane (RPI Research Product International). Sterile 1 mmol/L ammonium Fe(III) citrate (Sigma-Aldrich) was incubated with the iron-free siderophores at 1:1 (v/v) overnight at 4 ºC to obtain a 1 mmol/L siderophore stock solution at 50% saturation.

Plasmids.—All plasmids used in this study are listed in the Key Resource Table. Suicide plasmids were routinely propagated in DH5α λ*pir*. The flanking regions of the *B. thetaiotaomicron* genes BT_2063, BT_2065, BT_2063-65, BT_0496, BT_2479, BT2098-2100, BT_1950-52, BT_2409, BT_0502-04, BT_1219 were amplified and assembled into pExchange-tdk using the Gibson Assembly Cloning Kit (New England Biolab, Boston) to give rise to pWZ498, pWZ628, pWZ630, pWZ496, pWZ500, pWZ502, pWZ504, pWZ506, pWZ508, pWZ510, respectively. To complement the BT_2065 deletion, the flanking regions of the intergenic region between BT_3743 and BT_3744 were amplified and assembled into pExchange-tdk to give rise to pKI. Regions containing the promoter region and open reading frame of BT_2065 were amplified and assembled into pKI, yielding pWZ661. The flanking regions of the *E. coli entB* were amplified and ligated into pGP706 to generate pWZ517. The flanking regions of *S.* Typhimurium *iroB, fepA, cirA, iroN* genes were amplified and ligated into pGP706 to generate pWZ842, pWZ650, pWZ681, and pWZ626. *S.* Typhimurium *entB* was described previously (Tsolis et al., 1995) and was introduced into SL1344 by generalized phage transduction (Schmieger, 1972). Relevant plasmid inserts were verified by Sanger sequencing. In some instances, Nissle 1917 strains were marked by introducing the low-copy number plasmid pWSK129 through electroporation (WZ36 and WZ780) (Wang and Kushner, 1991).

Construction of mutants by allelic exchange.—All bacterial mutant strains constructed using the method below are listed in the Key Resource Table. For *B. thetaiotaomicron* mutants, suicide plasmid pExchange-tdk containing the flanking regions of genes of interest was conjugated into the *B. thetaiotaomicron* using S17-1 λ*pir* as the conjugative donor strain. Exconjugants that had the suicide plasmid integrated into the recipient chromosome (single crossover) were recovered on blood plates containing appropriate antibiotics. FudR plates (blood plates supplemented with 200 μg/mL 5-fluoro-2-deoxy-uridine) were used to select for the second crossover event. To create the *E. coli* Nissle 1917 *entB* mutant, pWZ517 was conjugated into the *E. coli* Nissle 1917 using S17-1 λ*pir*. Exconjugants that had the suicide plasmid integrated into the recipient chromosome (single crossover) were recovered on LB agar containing appropriate antibiotics. Sucrose plates (8 g/l nutrient broth base, 5 % sucrose, 15 g/l agar) were used to select for the second crossover event, thus creating WZ532. Deletion of the target gene was confirmed by PCR. Similar strategies were used to construct *S.* Typhimurium mutants lacking *iroB*, and *fepA cirA iroN*.

Transcriptional profiling of *B. thetaiotaomicron* in large intestine of gnotobiotic mice.—Total RNA of cecal contents was extracted and purified using RNeasy PowerMicrobiome Kit (Qiagen, CA) per the manufacturer's recommendations. TruSeq Stranded Total RNA Library Prep kit (Illumina, CA) with Ribo-Zero Gold ('epidemiology') was used to construct single-end 150 bp RNAseq libraries depleted of host and bacterial ribosomes. Quantity and quality of total RNA and final libraries was determined using a Qubit 3 (Thermo Fisher) and TapeStation 4200 (Agilent, CA), respectively, before sequencing on an Illumina NextSeq 500 (Illumina, CA). Reads were trimmed using BBMap software suite and decontaminated by filtering against mouse genome (mm10, UCSC Genome Browser). Mapping against the *B. thetaiotaomicron* genome VPI-5482 was performed using Bowtie2 (Langmead and Salzberg, 2012; Langmead et al., 2019). Mapped reads were quantified using featureCounts software package (Liao et al., 2014) and differential expression analysis was performed using DESeq2 software (Love et al., 2014).

Targeted quantification of mRNA levels in intestinal tissue and contents.—
Colonic or cecal tissue were homogenized in a bead beater (Biospec Products, Bartlesville) and RNA extracted using the TRI reagent method (Molecular Research Center, Cincinnati). DNA contamination was removed using the DNA-free Kit (Ambion, USA) per the manufacturer's recommendations. RNA from intestinal contents was extracted using the RNeasy PowerMicrobiome Kit (Qiagen, USA) per manufacturer's recommendation. TaqMan reverse transcription reagents (Invitrogen, USA) was used to generate cDNA. Real-time PCR was performed using Power SYBR Green Master Mix (Applied Biosystem, USA), data was acquired in a QuantStudio 6 Flex instrument (Life Technologies, USA). The final concentration of primers listed in Table S2 was 250 nM. Target gene transcription of each sample was normalized to the respective levels of *Gapdh* (mouse) or *gmk* (bacterial) mRNA.

Microbiota analysis.—RNA from the colon contents were extracted and reverse transcribed as described above. A 2 μl sample of the bacterial cDNA was used as the

template for SYBR-green based real-time PCR reactions as described above. The primers used in this experiment were listed in Table S2. The gene copy number in the sample was determined based on a standard curve generated by using pSW196, pSW325, and pSW326 (Bacchetti De Gregoris et al., 2011). Plasmid preparations with a known DNA concentration were diluted (100-fold serial dilutions) and the threshold cycle value (Ct) determined by qPCR as described above. These Ct values were used to generate a standard curve.

Quantification of *Bacteroides* populations.—Quantification of *B. thetaiotaomicron* was done by two independent methods. In a culture-independent method, we used qPCR to quantify the copy numbers of *B. thetaiotaomicron* genomes using primers specific for genome-inserted signature tags. In this method, BT_0159, whose deletion bears no fitness cost *in vitro* or *in vivo* (Goodman et al., 2009), was replaced with a nonfunctional chloramphenicol resistance cassette fused with unique signature tags (Potvin et al., 2003) to generate signature-tagged, isogenic wild-type strains (WZ412, WZ413, WZ415, WZ418, and WZ433). The signature tags and the corresponding detection primers are listed in Table S2. A variable primer that hybridizes to each unique 20 bp tag and a universal primer that hybridizes to a position in the chloramphenicol resistance cassette (224 bp away from the signature tag) were used to detect tagged genomes by qPCR. To ensure the specificity of each signature tag, genomic DNA from *B. thetaiotaomicron* strains harboring each of the five signature tags were combined in pre-determined ratios and tested for the specificity of the tags using RT-qPCR assays (data not shown). Targeted mutations of genes involved in iron uptake were made in the background of WZ412, WZ413, WZ415, WZ418, or WZ433, respectively, to generate WZ534, WZ537, WZ541, WZ549, WZ551, WZ553, WZ555, WZ591, WZ636, WZ647, and WZ697. To detect the relative representation of each strain *in vitro* and *in vivo*, bacterial genomic DNA were extracted by directly boiling bacterial suspension in sterile water or using the QIAamp PowerFecal DNA isolation kit (Qiagen, USA) per the recommendations of the manufacturer. Tagged genomes were detected using the qPCR method as described above. 2 μL of 100-fold serial diluted, purified plasmid DNA standards prepared from each tagged cassette were included in each qPCR run as described above. A standard curve was generated using these standards and used to calculate the relative representation of each strain in each sample. This method was used for experiments shown in Fig. 4C, **S3A**, and S5B–E. For all other experiments, a culture-dependent method was used. Wild-type *B. thetaiotaomicron* VPI-5482 (Xu et al., 2003) is resistant to gentamycin. To differentially mark the BT_2065 mutant (WZ777), a chloramphenicol resistant cassette derived from pACYC184 (Chang and Cohen, 1978) was inserted into the intergenic region of BT_3743 and BT_3744. Colonic or cecal contents were serially diluted in sterile PBS and plated on selective agar plates, followed by incubation in the anaerobic chamber. Colonization levels of mouse *Bacteroides* isolates were quantified using Gentamycin-supplemented blood agar plates as selective media.

Detection of enterobactin in intestinal contents.—Intestinal contents were harvested in sterile PBS and homogenized using Lysing Matrix B (MP Biomedicals, USA). The resulting supernatant was filter-sterilized and mixed with an equal volume of iron-limiting growth media (LB broth supplemented with 200 μmol/L BPS and 100 μmol/L Kanamycin) containing 2×10^4 CFU/ml of a reporter strain (*S*. Tm SL1344 *entB*). Sterile PBS or a serial

dilution of iron-laden enterobactin were used as controls. The incubation was allowed to proceed aerobically for 12 hours and growth of the reporter strain was determined by measuring optical density of the culture at 600 nm (OD_{600}).

Inductively Coupled Plasma Mass Spectrometry.—For measurement of intracellular iron concentration, 8–10 colonies of indicated strains were cultured in 3 ml of modified, semi-defined medium (1.5 g/L KH_2PO_4, 0.5 g/L NH_4SO_4, 0.9 g/L NaCl, 150 mg/L L-methionine, 5 μg/L vitamin B_{12}, 20 mg/L $MgCl_2 \times 6\ H_2O$, 10 mg/L $CaCl_2 \times 2\ H_2O$, 1 mg/L $MnCl_2 \times 4\ H_2O$, 1 mg/L $CoCl_2 \times 6\ H_2O$, 1 mg/L resazurin, 1 g/L L-cysteine, 5 mg/L protoporphyrin IX, 5 g/L glucose, 1 g/L tryptone, 0.2% $NaHCO_3$, and 200 μmol/L BPS, pH = 7.2) (Rocha and Smith, 2004) anaerobically for 24 hours, and subcultured (1:50) in 50 ml of modified semi-defined medium supplemented with 0.5 μmol/L iron-laden enterobactin for additional 36 hours before ICP-MS measurement. Cells were washed three times with 1 mM EDTA (pH = 8.0) to remove extracellular iron before acid digestion. For measurement of iron concentration in the large intestine, cecal contents were collected and the soluble and chelatable fractions were obtained by mixing the contents with H_2O and 1 mM EDTA (pH = 8.0) respectively. The iron in the remaining contents was considered the inaccessible fraction. After collection, the samples were digested using freshly prepared 50% nitric acid (Thermo Fisher Scientific, USA). Incubation in nitric acid was allowed to proceed for two days to ensure complete digestion of the cells and dissolution of the metals to be analyzed. Nitric acid was evaporated by heating the vials in an oil-bath at 150 °C in a chemical fume hood and the remaining matter in each vial was re-dissolved in 3% nitric acid followed by sonication for 30 min to ensure a homogeneous dispersion of the iron to be analyzed. The solution was then centrifuged and filtered if needed to remove any particulates. The supernatant was analyzed for iron by inductively coupled plasma mass spectrometry (ICP-MS) using Agilent 7700x instrument (Agilent Technologies). The measurement was repeated three times for each sample.

Measurement of free iron in the ferene-S assay—Working solution containing chromogenic reagent ferene-s ($NH_4CH_3CO_2$, 0.4 mol/L; (3-(2-Pyridyl)-5,6-di(2-furyl)1,2,4-triazine-5′,5′′-disulfonic acid disodium salt (Ferene-s), 0.005 mol/L; pH = 4.3) was prepared (Hedayati et al., 2018). 900 μL of working solution was mixed with 100 μL of sample and incubated at room temperature in the dark for 20 hours. Iron concentration was determined by measuring the absorbance at 595nm.

QUANTIFICATION AND STATISTICAL ANALYSIS.

Unless noted otherwise, data analysis was performed in GraphPad Prism v8.1.1. Values of bacterial population sizes, competitive indices, iron concentrations, and fold changes in mRNA levels were normally distributed after transformation by the natural logarithm. A two-tailed Student's t-test was then applied to the ln-transformed data. Unless otherwise stated, *, $P < 0.05$; **, $P < 0.01$; ***, $P < 0.001$; ns, not statistically significant. The exact number of independent samples (N) and other information regarding descriptive statistics, such as the definition of bar height and error bars, is listed in each figure legend. In all mouse experiments, N refers to the number of animals from which samples were taken. Sample sizes (e.g. the number of animals per group) were not estimated *a priori* since effect

sizes in our system cannot be predicted. No predicted statistical outliers were removed since the presence or absence of these potential statistical outliers did not affect the overall interpretation. Mice that were euthanized early due to health concerns were excluded from analysis.

DATA AND CODE AVAILABILITY

The sequencing data has been deposited in the European Nucleotide Archive under the accession number PRJEB33026.

Supplementary Material

Refer to Web version on PubMed Central for supplementary material.

ACKNOWLEDGEMENTS

REFERENCES

Anderson MT, Mitchell LA, Zhao L, and Mobley HLT (2017). Capsule Production and Glucose Metabolism Dictate Fitness during Serratia marcescens Bacteremia. MBio. 8(3). Published online 2017/05/26 DOI: 10.1128/mBio.00740-17.

Arpaia N, Campbell C, Fan X, Dikiy S, van der Veeken J, deRoos P, Liu H, Cross JR, Pfeffer K, Coffer PJ, et al. (2013). Metabolites produced by commensal bacteria promote peripheral regulatory T-cell generation. Nature. 504(7480), 451–455. Published online 2013/11/15 DOI: 10.1038/nature12726. [PubMed: 24226773]

Arthur JC, Perez-Chanona E, Muhlbauer M, Tomkovich S, Uronis JM, Fan TJ, Campbell BJ, Abujamel T, Dogan B, Rogers AB, et al. (2012). Intestinal inflammation targets cancer-inducing activity of the microbiota. Science. 338(6103), 120–123. Published online 2012/08/21 DOI: 10.1126/science.1224820. [PubMed: 22903521]

Bacchetti De Gregoris T, Aldred N, Clare AS, and Burgess JG (2011). Improvement of phylum- and class-specific primers for real-time PCR quantification of bacterial taxa. J Microbiol Methods. 86(3), 351–356. Published online 2011/06/28 DOI: 10.1016/j.mimet.2011.06.010. [PubMed: 21704084]

Baumler AJ, Norris TL, Lasco T, Voight W, Reissbrodt R, Rabsch W, and Heffron F. (1998). IroN, a novel outer membrane siderophore receptor characteristic of Salmonella enterica. J Bacteriol. 180(6), 1446–1453. Published online 1998/03/27. [PubMed: 9515912]

Caza M, and Kronstad JW (2013). Shared and distinct mechanisms of iron acquisition by bacterial and fungal pathogens of humans. Front Cell Infect Microbiol. 3, 80 Published online 2013/12/07 DOI: 10.3389/fcimb.2013.00080. [PubMed: 24312900]

Chang AC, and Cohen SN (1978). Construction and characterization of amplifiable multicopy DNA cloning vehicles derived from the P15A cryptic miniplasmid. J Bacteriol. 134(3), 1141–1156. Published online 1978/06/01. [PubMed: 149110]

Costa LF, Mol JP, Silva AP, Macedo AA, Silva TM, Alves GE, Winter S, Winter MG, Velazquez EM, Byndloss MX, et al. (2016). Iron acquisition pathways and colonization of the inflamed intestine by

Salmonella enterica serovar Typhimurium. Int J Med Microbiol. 306(8), 604–610. Published online 2016/10/21 DOI: 10.1016/j.ijmm.2016.10.004. [PubMed: 27760693]

Crouch ML, Castor M, Karlinsey JE, Kalhorn T, and Fang FC (2008). Biosynthesis and IroC-dependent export of the siderophore salmochelin are essential for virulence of Salmonella enterica serovar Typhimurium. Mol Microbiol. 67(5), 971–983. Published online 2008/01/16 DOI: 10.1111/j.1365-2958.2007.06089.x. [PubMed: 18194158]

Cullen TW, Schofield WB, Barry NA, Putnam EE, Rundell EA, Trent MS, Degnan PH., Booth CJ., Yu H., and Goodman AL. (2015). Gut microbiota. Antimicrobial peptide resistance mediates resilience of prominent gut commensals during inflammation. Science. 347(6218), 170–175. Published online 2015/01/13 DOI: 10.1126/science.1260580. [PubMed: 25574022]

Curtis MM, Hu Z, Klimko C, Narayanan S, Deberardinis R, and Sperandio V. (2014). The gut commensal Bacteroides thetaiotaomicron exacerbates enteric infection through modification of the metabolic landscape. Cell Host Microbe. 16(6), 759–769. Published online 2014/12/17 DOI: 10.1016/j.chom.2014.11.005. [PubMed: 25498343]

Degnan PH, Barry NA, Mok KC, Taga ME, and Goodman AL (2014). Human gut microbes use multiple transporters to distinguish vitamin B(1)(2) analogs and compete in the gut. Cell Host Microbe. 15(1), 47–57. Published online 2014/01/21 DOI: 10.1016/j.chom.2013.12.007. [PubMed: 24439897]

Deriu E, Liu JZ, Pezeshki M, Edwards RA, Ochoa RJ, Contreras H, Libby SJ, Fang FC, and Raffatellu M. (2013). Probiotic bacteria reduce salmonella typhimurium intestinal colonization by competing for iron. Cell Host Microbe. 14(1), 26–37. Published online 2013/07/23 DOI: 10.1016/j.chom.2013.06.007. [PubMed: 23870311]

Desai MS, Seekatz AM, Koropatkin NM, Kamada N, Hickey CA, Wolter M, Pudlo NA, Kitamoto S, Terrapon N, Muller A, et al. (2016). A Dietary FiberDeprived Gut Microbiota Degrades the Colonic Mucus Barrier and Enhances Pathogen Susceptibility. Cell. 167(5), 1339–1353 e1321 Published online 2016/11/20 DOI: 10.1016/j.cell.2016.10.043. [PubMed: 27863247]

Diaz-Ochoa VE, Lam D, Lee CS, Klaus S, Behnsen J, Liu JZ, Chim N, Nuccio SP, Rathi SG, Mastroianni JR, et al. (2016). Salmonella Mitigates Oxidative Stress and Thrives in the Inflamed Gut by Evading Calprotectin-Mediated Manganese Sequestration. Cell Host Microbe. 19(6), 814–825. Published online 2016/06/10 DOI: 10.1016/j.chom.2016.05.005. [PubMed: 27281571]

Endt K, Stecher B, Chaffron S, Slack E, Tchitchek N, Benecke A, Van Maele L, Sirard JC, Mueller AJ, Heikenwalder M, et al. (2010). The microbiota mediates pathogen clearance from the gut lumen after non-typhoidal Salmonella diarrhea. PLoS Pathog. 6(9), e1001097 Published online 2010/09/17 DOI: 10.1371/journal.ppat.1001097.

Faith JJ, Guruge JL, Charbonneau M, Subramanian S, Seedorf H, Goodman AL, Clemente JC, Knight R, Heath AC, Leibel RL, et al. (2013). The long-term stability of the human gut microbiota. Science. 341(6141), 1237439 Published online 2013/07/06 DOI: 10.1126/science.1237439.

Fischbach MA, and Sonnenburg JL (2011). Eating for two: how metabolism establishes interspecies interactions in the gut. Cell Host Microbe. 10(4), 336–347. Published online 2011/10/25 DOI: 10.1016/j.chom.2011.10.002. [PubMed: 22018234]

Frost GE, and Rosenberg H. (1975). Relationship between the tonB locus and iron transport in Escherichia coli. J Bacteriol. 124(2), 704–712. Published online 1975/11/01. [PubMed: 126991]

Garrett WS, Gallini CA, Yatsunenko T, Michaud M, DuBois A, Delaney ML, Punit S, Karlsson M, Bry L, Glickman JN, et al. (2010). Enterobacteriaceae act in concert with the gut microbiota to induce spontaneous and maternally transmitted colitis. Cell Host Microbe. 8(3), 292–300. DOI: 10.1016/j.chom.2010.08.004. [PubMed: 20833380]

Goodman AL, McNulty NP, Zhao Y, Leip D, Mitra RD, Lozupone CA, Knight R, and Gordon JI (2009). Identifying genetic determinants needed to establish a human gut symbiont in its habitat. Cell Host Microbe. 6(3), 279–289. Published online 2009/09/15 DOI: 10.1016/j.chom.2009.08.003. [PubMed: 19748469]

Gunderson LH (2000). Ecological resilience - in theory and application. Annu Rev Ecol Syst. 31, 425–439. DOI: DOI 10.1146/annurev.ecolsys.31.1.425.

Hale LP, Gottfried MR, and Swidsinski A. (2005). Piroxicam treatment of IL-10-deficient mice enhances colonic epithelial apoptosis and mucosal exposure to intestinal bacteria. Inflamm Bowel

Dis. 11(12), 1060–1069. Published online 2005/11/25 DOI: 10.1097/01.mib.0000187582.90423.bc. [PubMed: 16306768]

Hantke K, Nicholson G, Rabsch W, and Winkelmann G. (2003). Salmochelins, siderophores of Salmonella enterica and uropathogenic Escherichia coli strains, are recognized by the outer membrane receptor IroN. Proc Natl Acad Sci U S A. 100(7), 3677–3682. Published online 2003/03/26 DOI: 10.1073/pnas.0737682100. [PubMed: 12655053]

Hedayati M, Abubaker-Sharif B, Khattab M, Razavi A, Mohammed I, Nejad A, Wabler M, Zhou H, Mihalic J, Gruettner C, et al. (2018). An optimised spectrophotometric assay for convenient and accurate quantitation of intracellular iron from iron oxide nanoparticles. Int J Hyperthermia. 34(4), 373–381. Published online 2017/08/02 DOI: 10.1080/02656736.2017.1354403. [PubMed: 28758530]

Hider RC, and Kong X. (2010). Chemistry and biology of siderophores. Nat Prod Rep. 27(5), 637–657. Published online 2010/04/09 DOI: 10.1039/b906679a. [PubMed: 20376388]

Hood MI, and Skaar EP (2012). Nutritional immunity: transition metals at the pathogen-host interface. Nat Rev Microbiol. 10(8), 525–537. Published online 2012/07/17 DOI: 10.1038/nrmicro2836. [PubMed: 22796883]

Jacobson A, Lam L, Rajendram M, Tamburini F, Honeycutt J, Pham T, Van Treuren W, Pruss K, Stabler SR, Lugo K, et al. (2018). A Gut Commensal-Produced Metabolite Mediates Colonization Resistance to Salmonella Infection. Cell Host Microbe. 24(2), 296–307 e297 Published online 2018/07/31 DOI: 10.1016/j.chom.2018.07.002. [PubMed: 30057174]

Karlinsey JE, Stepien TA, Mayho M, Singletary LA, Bingham-Ramos LK, Brehm MA, Greiner DL, Shultz LD, Gallagher LA, Bawn M, et al. (2019). Genome-wide Analysis of Salmonella enterica serovar Typhi in Humanized Mice Reveals Key Virulence Features. Cell Host Microbe. 26(3), 426–434 e426 Published online 2019/08/27 DOI: 10.1016/j.chom.2019.08.001. [PubMed: 31447308]

Klebba PE, McIntosh MA, and Neilands JB (1982). Kinetics of biosynthesis of iron-regulated membrane proteins in Escherichia coli. J Bacteriol. 149(3), 880–888. Published online 1982/03/01. [PubMed: 6174499]

Kruis W, Fric P, Pokrotnieks J, Lukas M, Fixa B, Kascak M, Kamm MA, Weismueller J, Beglinger C, Stolte M, et al. (2004). Maintaining remission of ulcerative colitis with the probiotic Escherichia coli Nissle 1917 is as effective as with standard mesalazine. Gut. 53(11), 1617–1623. Published online 2004/10/14 DOI: 10.1136/gut.2003.037747. [PubMed: 15479682]

Kruis W, Schutz E, Fric P, Fixa B, Judmaier G, and Stolte M. (1997). Double-blind comparison of an oral Escherichia coli preparation and mesalazine in maintaining remission of ulcerative colitis. Aliment Pharmacol Ther. 11(5), 853–858. Published online 1997/11/14. [PubMed: 9354192]

Langmead B, and Salzberg SL (2012). Fast gapped-read alignment with Bowtie 2. Nat Methods. 9(4), 357–359. Published online 2012/03/06 DOI: 10.1038/nmeth.1923. [PubMed: 22388286]

Langmead B, Wilks C, Antonescu V, and Charles R. (2019). Scaling read aligners to hundreds of threads on general-purpose processors. Bioinformatics. 35(3), 421–432. Published online 2018/07/19 DOI: 10.1093/bioinformatics/bty648. [PubMed: 30020410]

Lauber F, Cornelis GR, and Renzi F. (2016). Identification of a New Lipoprotein Export Signal in Gram-Negative Bacteria. MBio. 7(5). Published online 2016/11/01 DOI: 10.1128/mBio.01232-16.

Lee SM, Donaldson GP, Mikulski Z, Boyajian S, Ley K, and Mazmanian SK (2013). Bacterial colonization factors control specificity and stability of the gut microbiota. Nature. 501(7467), 426–429. Published online 2013/08/21 DOI: 10.1038/nature12447. [PubMed: 23955152]

Liao Y, Smyth GK, and Shi W. (2014). featureCounts: an efficient general purpose program for assigning sequence reads to genomic features. Bioinformatics. 30(7), 923–930. Published online 2013/11/15 DOI: 10.1093/bioinformatics/btt656. [PubMed: 24227677]

Lim B, Zimmermann M, Barry NA, and Goodman AL (2017). Engineered Regulatory Systems Modulate Gene Expression of Human Commensals in the Gut. Cell. 169(3), 547–558 e515 Published online 2017/04/22 DOI: 10.1016/j.cell.2017.03.045. [PubMed: 28431252]

Lopez CA, and Skaar EP (2018). The Impact of Dietary Transition Metals on Host-Bacterial Interactions. Cell Host Microbe. 23(6), 737–748. Published online 2018/06/15 DOI: 10.1016/j.chom.2018.05.008. [PubMed: 29902439]

Love MI, Huber W, and Anders S. (2014). Moderated estimation of fold change and dispersion for RNA-seq data with DESeq2. Genome Biol. 15(12), 550 Published online 2014/12/18 DOI: 10.1186/s13059-014-0550-8. [PubMed: 25516281]

Lozupone CA, Stombaugh JI, Gordon JI, Jansson JK, and Knight R. (2012). Diversity, stability and resilience of the human gut microbiota. Nature. 489(7415), 220–230. Published online 2012/09/14 DOI: 10.1038/nature11550. [PubMed: 22972295]

Luke RK, and Gibson F. (1971). Location of three genes concerned with the conversion of 2,3-dihydroxybenzoate into enterochelin in Escherichia coli K-12. J Bacteriol. 107(2), 557–562. Published online 1971/08/01. [PubMed: 4939766]

Lupp C, Robertson ML, Wickham ME, Sekirov I, Champion OL, Gaynor EC, and Finlay BB (2007). Host-mediated inflammation disrupts the intestinal microbiota and promotes the overgrowth of Enterobacteriaceae. Cell Host Microbe. 2(2), 119–129. Published online 2007/11/17 DOI: 10.1016/j.chom.2007.06.010. [PubMed: 18005726]

Luu M, Weigand K, Wedi F, Breidenbend C, Leister H, Pautz S, Adhikary T, and Visekruna A. (2018). Regulation of the effector function of CD8(+) T cells by gut microbiota-derived metabolite butyrate. Sci Rep. 8(1), 14430 Published online 2018/09/28 DOI: 10.1038/s41598-018-32860-x. [PubMed: 30258117]

Manfredi P, Lauber F, Renzi F, Hack K, Hess E, and Cornelis GR (2015). New iron acquisition system in Bacteroidetes. Infect Immun. 83(1), 300–310. Published online 2014/11/05 DOI: 10.1128/IAI.02042-14. [PubMed: 25368114]

Martens EC, Chiang HC, and Gordon JI (2008). Mucosal glycan foraging enhances fitness and transmission of a saccharolytic human gut bacterial symbiont. Cell Host Microbe. 4(5), 447–457. Published online 2008/11/11 DOI: 10.1016/j.chom.2008.09.007. [PubMed: 18996345]

Martens EC, Kelly AG, Tauzin AS, and Brumer H. (2014). The devil lies in the details: how variations in polysaccharide fine-structure impact the physiology and evolution of gut microbes. J Mol Biol. 426(23), 3851–3865. Published online 2014/07/16 DOI: 10.1016/j.jmb.2014.06.022. [PubMed: 25026064]

Mitsuoka T, and Hayakawa K. (1973). [The fecal flora in man. I. Composition of the fecal flora of various age groups]. Zentralbl Bakteriol Orig A. 223(2), 333–342. Published online 1973/03/01. [PubMed: 4145840]

Muller SI, Valdebenito M, and Hantke K. (2009). Salmochelin, the long-overlooked catecholate siderophore of Salmonella. Biometals. 22(4), 691–695. Published online 2009/02/14 DOI: 10.1007/s10534-009-9217-4. [PubMed: 19214756]

Muniz LR, Knosp C, and Yeretssian G. (2012). Intestinal antimicrobial peptides during homeostasis, infection, and disease. Front Immunol. 3, 310 Published online 2012/10/23 DOI: 10.3389/fimmu.2012.00310. [PubMed: 23087688]

Nagy TA, Moreland SM, Andrews-Polymenis H, and Detweiler CS (2013). The ferric enterobactin transporter Fep is required for persistent Salmonella enterica serovar typhimurium infection. Infect Immun. 81(11), 4063–4070. Published online 2013/08/21 DOI: 10.1128/IAI.00412-13. [PubMed: 23959718]

Nagy TA, Moreland SM, and Detweiler CS (2014). Salmonella acquires ferrous iron from haemophagocytic macrophages. Mol Microbiol. 93(6), 1314–1326. Published online 2014/08/02 DOI: 10.1111/mmi.12739. [PubMed: 25081030]

Otto BR, Sparrius M, Verweij-van Vught AM, and MacLaren DM (1990). Iron-regulated outer membrane protein of Bacteroides fragilis involved in heme uptake. Infect Immun. 58(12), 3954–3958. Published online 1990/12/01. [PubMed: 2254022]

Penders J, Thijs C, Vink C, Stelma FF, Snijders B, Kummeling I, van den Brandt PA, and Stobberingh EE (2006). Factors influencing the composition of the intestinal microbiota in early infancy. Pediatrics. 118(2), 511–521. Published online 2006/08/03 DOI: 10.1542/peds.2005-2824. [PubMed: 16882802]

Pham TA, and Lawley TD (2014). Emerging insights on intestinal dysbiosis during bacterial infections. Curr Opin Microbiol. 17, 67–74. Published online 2014/03/04 DOI: 10.1016/j.mib.2013.12.002. [PubMed: 24581695]

Pollack JR, and Neilands JB (1970). Enterobactin, an iron transport compound from Salmonella typhimurium. Biochem Biophys Res Commun. 38(5), 989–992. Published online 1970/03/12 DOI: 10.1016/0006-291x(70)90819-3. [PubMed: 4908541]

Potvin E, Lehoux DE, Kukavica-Ibrulj I, Richard KL, Sanschagrin F, Lau GW, and Levesque RC (2003). In vivo functional genomics of Pseudomonas aeruginosa for high-throughput screening of new virulence factors and antibacterial targets. Environ Microbiol. 5(12), 1294–1308. Published online 2003/12/03. [PubMed: 14641575]

Pugsley AP, and Reeves P. (1976). Iron uptake in colicin B-resistant mutants of Escherichia coli K-12. J Bacteriol. 126(3), 1052–1062. Published online 1976/06/01. [PubMed: 7543]

Rabsch W, Methner U, Voigt W, Tschape H, Reissbrodt R, and Williams PH (2003). Role of receptor proteins for enterobactin and 2,3-dihydroxybenzoylserine in virulence of Salmonella enterica. Infect Immun. 71(12), 6953–6961. Published online 2003/11/26 DOI: 10.1128/iai.71.12.6953-6961.2003. [PubMed: 14638784]

Rabsch W, Voigt W, Reissbrodt R, Tsolis RM, and Baumler AJ (1999). Salmonella typhimurium IroN and FepA proteins mediate uptake of enterobactin but differ in their specificity for other siderophores. J Bacteriol. 181(11), 3610–3612. Published online 1999/05/29. [PubMed: 10348879]

Raffatellu M, George MD, Akiyama Y, Hornsby MJ, Nuccio SP, Paixao TA, Butler BP, Chu H, Santos RL, Berger T, et al. (2009). Lipocalin-2 resistance confers an advantage to Salmonella enterica serotype Typhimurium for growth and survival in the inflamed intestine. Cell Host Microbe. 5(5), 476–486. Published online 2009/05/21 DOI: 10.1016/j.chom.2009.03.011. [PubMed: 19454351]

Rembacken BJ, Snelling AM, Hawkey PM, Chalmers DM, and Axon AT (1999). Non-pathogenic Escherichia coli versus mesalazine for the treatment of ulcerative colitis: a randomised trial. Lancet. 354(9179), 635–639. Published online 1999/08/31 DOI: 10.1016/s0140-6736(98)06343-0. [PubMed: 10466665]

Rocha ER, de Uzeda M, and Brock JH (1991). Effect of ferric and ferrous iron chelators on growth of Bacteroides fragilis under anaerobic conditions. FEMS Microbiol Lett. 68(1), 45–50. Published online 1991/11/01 DOI: 10.1016/0378-1097(91)90393-o. [PubMed: 1769555]

Rocha ER, and Krykunivsky AS (2017). Anaerobic utilization of Fe(III)-xenosiderophores among Bacteroides species and the distinct assimilation of Fe(III)-ferrichrome by Bacteroides fragilis within the genus. Microbiologyopen. 6(4). Published online 2017/04/12 DOI: 10.1002/mbo3.479.

Rocha ER, and Smith CJ (2004). Transcriptional regulation of the Bacteroides fragilis ferritin gene (ftnA) by redox stress. Microbiology. 150(Pt 7), 2125–2134. Published online 2004/07/17 DOI: 10.1099/mic.0.26948-0. [PubMed: 15256555]

Sassone-Corsi M, Chairatana P, Zheng T, Perez-Lopez A, Edwards RA, George MD, Nolan EM, and Raffatellu M. (2016). Siderophore-based immunization strategy to inhibit growth of enteric pathogens. Proc Natl Acad Sci U S A. 113(47), 13462–13467. Published online 2016/11/09 DOI: 10.1073/pnas.1606290113. [PubMed: 27821741]

Schmieger H. (1972). Phage P22-mutants with increased or decreased transduction abilities. Mol Gen Genet. 119(1), 75–88. Published online 1972/01/01 DOI: 10.1007/bf00270447. [PubMed: 4564719]

Skare JT, Ahmer BM, Seachord CL, Darveau RP, and Postle K (1993). Energy transduction between membranes. TonB, a cytoplasmic membrane protein, can be chemically cross-linked in vivo to the outer membrane receptor FepA. J Biol Chem. 268(22), 16302–16308. Published online 1993/08/05. [PubMed: 8344918]

Sommer F, Anderson JM, Bharti R, Raes J, and Rosenstiel P. (2017). The resilience of the intestinal microbiota influences health and disease. Nat Rev Microbiol. 15(10), 630–638. Published online 2017/06/20 DOI: 10.1038/nrmicro.2017.58. [PubMed: 28626231]

Sonnenborn U. (2016). Escherichia coli strain Nissle 1917-from bench to bedside and back: history of a special Escherichia coli strain with probiotic properties. FEMS Microbiol Lett. 363(19). Published online 2016/09/14 DOI: 10.1093/femsle/fnw212.

Sorbara MT, Dubin K, Littmann ER, Moody TU, Fontana E, Seok R, Leiner IM, Taur Y, Peled JU, van den Brink MRM, et al. (2019). Inhibiting antibiotic-resistant Enterobacteriaceae by microbiota-mediated intracellular acidification. J Exp Med. 216(1), 84–98. Published online 2018/12/20 DOI: 10.1084/jem.20181639. [PubMed: 30563917]

Spanogiannopoulos P, and Turnbaugh PJ (2018). Broad collateral damage of drugs against the gut microbiome. Nat Rev Gastroenterol Hepatol. 15(8), 457–458. Published online 2018/05/13 DOI: 10.1038/s41575-018-0028-3. [PubMed: 29752457]

Stecher B, Robbiani R, Walker AW, Westendorf AM, Barthel M, Kremer M, Chaffron S, Macpherson AJ, Buer J, Parkhill J, et al. (2007). Salmonella enterica serovar typhimurium exploits inflammation to compete with the intestinal microbiota. PLoS Biol. 5(10), 2177–2189. Published online 2007/09/01 DOI: 10.1371/journal.pbio.0050244. [PubMed: 17760501]

Tamboli CP, Neut C, Desreumaux P, and Colombel JF (2004). Dysbiosis in inflammatory bowel disease. Gut. 53(1), 1–4. Published online 2003/12/20. [PubMed: 14684564]

Tsolis RM, Baumler AJ, Stojiljkovic I, and Heffron F. (1995). Fur regulon of Salmonella typhimurium: identification of new iron-regulated genes. J Bacteriol. 177(16), 4628–4637. Published online 1995/08/01 DOI: 10.1128/jb.177.16.4628-4637.1995. [PubMed: 7642488]

Verweijvanvught AMJJ, Otto BR, Namavar F, Sparrius M, and Maclaren DM (1988). Ability of Bacteroides Species to Obtain Iron from Iron Salts, Heme-Compounds and Transferrin. Fems Microbiology Letters. 49(2), 223–228.

Wang RF, and Kushner SR (1991). Construction of versatile low-copy-number vectors for cloning, sequencing and gene expression in Escherichia coli. Gene. 100, 195–199. Published online 1991/04/01. [PubMed: 2055470]

Wexler AG, Schofield WB, Degnan PH, Folta-Stogniew E, Barry NA, and Goodman AL (2018). Human gut Bacteroides capture vitamin B12 via cell surface-exposed lipoproteins. Elife. 7. Published online 2018/09/19 DOI: 10.7554/eLife.37138.

Winter SE, and Baumler AJ (2014). Dysbiosis in the inflamed intestine: chance favors the prepared microbe. Gut Microbes. 5(1), 71–73. Published online 2014/03/19 DOI: 10.4161/gmic.27129. [PubMed: 24637596]

Winter SE, Winter MG, Xavier MN, Thiennimitr P, Poon V, Keestra AM, Laughlin RC, Gomez G, Wu J, Lawhon SD, et al. (2013). Host-derived nitrate boosts growth of E. coli in the inflamed gut. Science. 339(6120), 708–711. Published online 2013/02/09 DOI: 10.1126/science.1232467. [PubMed: 23393266]

Wong SH, Zhao L, Zhang X, Nakatsu G, Han J, Xu W, Xiao X, Kwong TNY, Tsoi H, Wu WKK, et al. (2017). Gavage of Fecal Samples From Patients With Colorectal Cancer Promotes Intestinal Carcinogenesis in Germ-Free and Conventional Mice. Gastroenterology. 153(6), 1621–1633 e1626 Published online 2017/08/22 DOI: 10.1053/j.gastro.2017.08.022. [PubMed: 28823860]

Wookey P, and Rosenberg H. (1978). Involvement of inner and outer membrane components in the transport of iron and in colicin B action in Escherichia coli. J Bacteriol. 133(2), 661–666. Published online 1978/02/01. [PubMed: 146699]

Xu J, Bjursell MK, Himrod J, Deng S, Carmichael LK, Chiang HC, Hooper LV, and Gordon JI (2003). A genomic view of the human-Bacteroides thetaiotaomicron symbiosis. Science. 299(5615), 2074–2076. Published online 2003/03/29 DOI: 10.1126/science.1080029. [PubMed: 12663928]

Yep A, McQuade T, Kirchhoff P, Larsen M, and Mobley HL (2014). Inhibitors of TonB function identified by a high-throughput screen for inhibitors of iron acquisition in uropathogenic Escherichia coli CFT073. MBio. 5(2), e01089–01013 Published online 2014/02/27 DOI: 10.1128/mBio.01089-13.

Young IG, Langman L, Luke RK, and Gibson F (1971). Biosynthesis of the iron-transport compound enterochelin: mutants of Escherichia coli unable to synthesize 2,3-dihydroxybenzoate. J Bacteriol. 106(1), 51–57. Published online 1971/04/01. [PubMed: 4928016]

Zhu W, Miyata N, Winter MG, Arenales A, Hughes ER, Spiga L, Kim J, Sifuentes-Dominguez L, Starokadomskyy P, Gopal P, et al. (2019a). Editing of the gut microbiota reduces carcinogenesis in mouse models of colitis-associated colorectal cancer. J Exp Med. Published online 2019/07/31 DOI: 10.1084/jem.20181939.

Zhu W, Spiga L, and Winter S. (2019b). Transition metals and host-microbe interactions in the inflamed intestine. Biometals. Published online 2019/02/23 DOI: 10.1007/s10534-019-00182-8.

Zhu W, Winter MG, Byndloss MX, Spiga L, Duerkop BA, Hughes ER, Buttner L, de Lima Romao E, Behrendt CL, Lopez CA, et al. (2018). Precision editing of the gut microbiota ameliorates colitis.

Nature. 553(7687), 208–211. Published online 2018/01/13 DOI: 10.1038/nature25172. [PubMed: 29323293]

Bacchetti De Gregoris T, Aldred N, Clare AS, and Burgess JG (2011). Improvement of phylum- and class-specific primers for real-time PCR quantification of bacterial taxa. J Microbiol Methods. 86(3), 351–356. Published online 2011/06/28 DOI: 10.1016/j.mimet.2011.06.010. [PubMed: 21704084]

Barman M, Unold D, Shifley K, Amir E, Hung K, Bos N, and Salzman N. (2008). Enteric salmonellosis disrupts the microbial ecology of the murine gastrointestinal tract. Infect Immun. 76(3), 907–915. Published online 2007/12/28 DOI: 10.1128/IAI.01432-07. [PubMed: 18160481]

Gillis CC, Winter MG, Chanin RB, Zhu W, Spiga L, and Winter SE (2019). Host-derived metabolites modulate transcription of Salmonella genes involved in l-lactate utilization during gut colonization. Infect Immun. Published online 2019/01/09 DOI: 10.1128/IAI.00773-18.

Godinez I, Haneda T, Raffatellu M, George MD, Paixao TA, Rolan HG, Santos RL, Dandekar S, Tsolis RM, and Baumler AJ (2008). T cells help to amplify inflammatory responses induced by Salmonella enterica serotype Typhimurium in the intestinal mucosa. Infect Immun. 76(5), 2008–2017. Published online 2008/03/19 DOI: 10.1128/IAI.01691-07. [PubMed: 18347048]

Grozdanov L, Raasch C, Schulze J, Sonnenborn U, Gottschalk G, Hacker J, and Dobrindt U. (2004). Analysis of the genome structure of the nonpathogenic probiotic Escherichia coli strain Nissle 1917. J Bacteriol. 186(16), 5432–5441. Published online 2004/08/05 DOI: 10.1128/JB.186.16.5432-5441.2004. [PubMed: 15292145]

Hoiseth SK, and Stocker BA (1981). Aromatic-dependent Salmonella typhimurium are non-virulent and effective as live vaccines. Nature. 291(5812), 238–239. Published online 1981/05/21. [PubMed: 7015147]

Hughes ER, Winter MG, Duerkop BA, Spiga L, Furtado de Carvalho T, Zhu W, Gillis CC, Buttner L, Smoot MP, Behrendt CL, et al. (2017). Microbial Respiration and Formate Oxidation as Metabolic Signatures of Inflammation-Associated Dysbiosis. Cell Host Microbe. 21(2), 208–219. Published online 2017/02/10 DOI: 10.1016/j.chom.2017.01.005. [PubMed: 28182951]

Koropatkin NM, Martens EC, Gordon JI, and Smith TJ (2008). Starch catabolism by a prominent human gut symbiont is directed by the recognition of amylose helices. Structure. 16(7), 1105–1115. Published online 2008/07/10 DOI: 10.1016/j.str.2008.03.017. [PubMed: 18611383]

Langmead B, and Salzberg SL (2012). Fast gapped-read alignment with Bowtie 2. Nat Methods. 9(4), 357–359. Published online 2012/03/06 DOI: 10.1038/nmeth.1923. [PubMed: 22388286]

Liao Y, Smyth GK, and Shi W. (2014). featureCounts: an efficient general purpose program for assigning sequence reads to genomic features. Bioinformatics. 30(7), 923–930. Published online 2013/11/15 DOI: 10.1093/bioinformatics/btt656. [PubMed: 24227677]

Liu JZ, Jellbauer S, Poe AJ, Ton V, Pesciaroli M, Kehl-Fie TE, Restrepo NA, Hosking MP, Edwards RA, Battistoni A, et al. (2012). Zinc sequestration by the neutrophil protein calprotectin enhances Salmonella growth in the inflamed gut. Cell Host Microbe. 11(3), 227–239. Published online 2012/03/20 DOI: 10.1016/j.chom.2012.01.017. [PubMed: 22423963]

Love MI, Huber W, and Anders S. (2014). Moderated estimation of fold change and dispersion for RNA-seq data with DESeq2. Genome Biol. 15(12), 550 Published online 2014/12/18 DOI: 10.1186/s13059-014-0550-8. [PubMed: 25516281]

Overbergh L, Giulietti A, Valckx D, Decallonne R, Bouillon R, and Mathieu C. (2003). The use of real-time reverse transcriptase PCR for the quantification of cytokine gene expression. J Biomol Tech. 14(1), 33–43. Published online 2003/08/07. [PubMed: 12901609]

Pal D, Venkova-Canova T, Srivastava P, and Chattoraj DK (2005). Multipartite regulation of rctB, the replication initiator gene of Vibrio cholerae chromosome II. J Bacteriol. 187(21), 7167–7175. Published online 2005/10/21 DOI: 10.1128/JB.187.21.7167-7175.2005. [PubMed: 16237000]

Potvin E, Lehoux DE, Kukavica-Ibrulj I, Richard KL, Sanschagrin F, Lau GW, and Levesque RC (2003). In vivo functional genomics of Pseudomonas aeruginosa for high-throughput screening of new virulence factors and antibacterial targets. Environ Microbiol. 5(12), 1294–1308. Published online 2003/12/03. [PubMed: 14641575]

Rudi K, Skulberg OM, Larsen F, and Jakobsen KS (1997). Strain characterization and classification of oxyphotobacteria in clone cultures on the basis of 16S rRNA sequences from the variable regions

V6, V7, and V8. Appl Environ Microbiol. 63(7), 2593–2599. Published online 1997/07/01. [PubMed: 9212409]

Simon R, Priefer U, and Puhler A. (1983). A Broad Host Range Mobilization System for In Vivo Genetic Engineering: Transposon Mutagenesis in Gram Negative Bacteria. Nature Biotechnology. 1, 784–791. DOI: doi:10.1038/nbt1183-784.

Spiga L, Winter MG, Carvalho TF, Zhu W, Hughes ER, Gillis CC, Behrendt CL, Kim J, Chessa D, Andrews-Polymenis H, et al. (2017). An oxidative central metabolism enables Salmonella to utilize microbiota-derived succinate. Cell Host Microbe. In press.

Stojiljkovic I, Baumler AJ, and Heffron F. (1995). Ethanolamine utilization in Salmonella typhimurium: nucleotide sequence, protein expression, and mutational analysis of the cchA cchB eutE eutJ eutG eutH gene cluster. J Bacteriol. 177(5), 1357–1366. Published online 1995/03/01 DOI: 10.1128/jb.177.5.1357-1366.1995. [PubMed: 7868611]

Tsolis RM, Baumler AJ, Stojiljkovic I, and Heffron F. (1995). Fur regulon of Salmonella typhimurium: identification of new iron-regulated genes. J Bacteriol. 177(16), 4628–4637. Published online 1995/08/01. [PubMed: 7642488]

Wang RF, and Kushner SR (1991). Construction of versatile low-copy-number vectors for cloning, sequencing and gene expression in Escherichia coli. Gene. 100, 195–199. Published online 1991/04/01. [PubMed: 2055470]

Wilson RP, Raffatellu M, Chessa D, Winter SE, Tukel C, and Baumler AJ (2008). The Vi-capsule prevents Toll-like receptor 4 recognition of Salmonella. Cell Microbiol. 10(4), 876–890. Published online 2007/11/24 DOI: 10.1111/j.1462-5822.2007.01090.x. [PubMed: 18034866]

Winter SE, Winter MG, Xavier MN, Thiennimitr P, Poon V, Keestra AM, Laughlin RC, Gomez G, Wu J, Lawhon SD, et al. (2013). Host-derived nitrate boosts growth of E. coli in the inflamed gut. Science. 339(6120), 708–711. Published online 2013/02/09 DOI: 10.1126/science.1232467. [PubMed: 23393266]

Author Manuscript

Author Manuscript

Author Manuscript

Author Manuscript

Highlights:

- Microbial access to the micronutrient iron is decreased during gut inflammation

- *Bacteroides thetaiotaomicron* acquires iron through siderophores from other bacteria.

- XusABC system is required for *B. thetaiotaomicron* to use enterobactin and salmochelin

- Xenosiderophores are critical for *B. thetaiotaomicron* colonization during inflammation
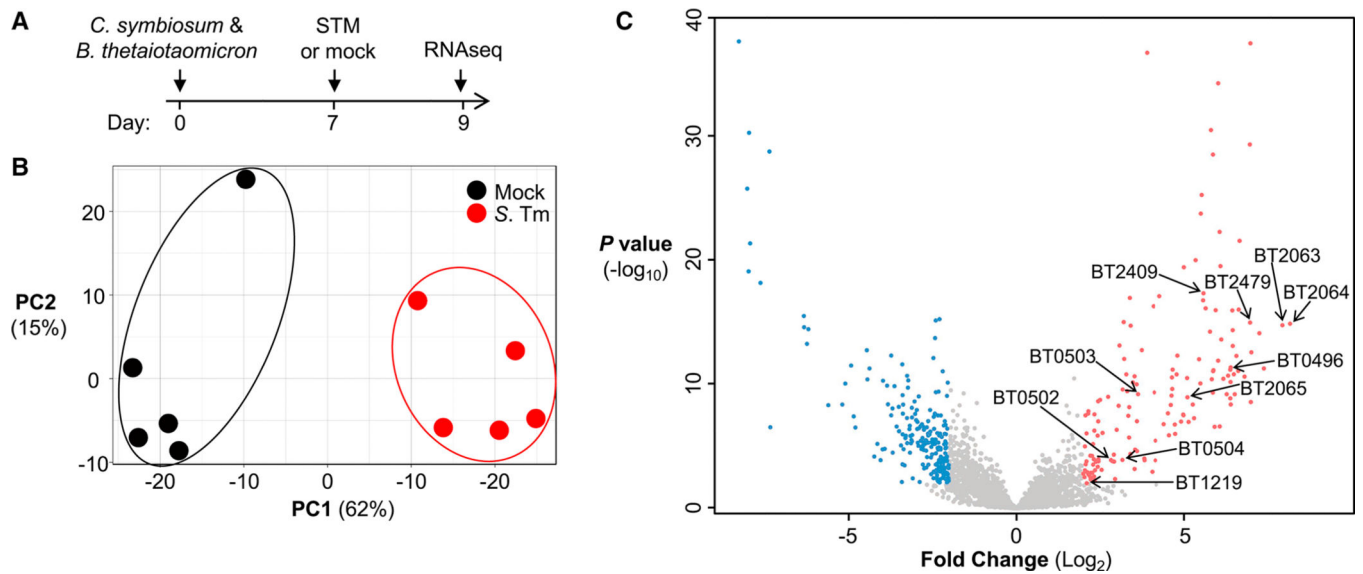
Figure 1: Changes in the *B. thetaiotaomicron* transcriptome in response to *Salmonella* infection.
(**A – C**) Groups of gnotobiotic Swiss Webster mice were colonized with *C. symbiosum* ATCC14940 and *B. thetaiotaomicron* VPI-5482 Δ*tdk* for 7 days. Mice were either intragastrically inoculated with *S.* Tm IR715 (*N* = 5) or remained uninfected (*N* = 5) for 2 days, and the cecal content was collected and the bacterial transcriptome assessed using RNA-seq. (**A**) Schematic representation of the experiment. (**B**) Principle coordinate plot of the *B. thetaiotaomicron* transcriptomes in mock-treated (black circles) and *S.* Tm-infected mice (red). (**C**) Volcano plot of differentially expressed genes in *B. thetaiotaomicron* in response to *S.* Tm infection. Genes downregulated by more than a 4-fold and *P* < 0.05 are shown in blue, genes upregulated by the same criteria are shown in red. Gene with predicted functions in iron metabolism are indicated by their gene locus number. See also Fig. S3.
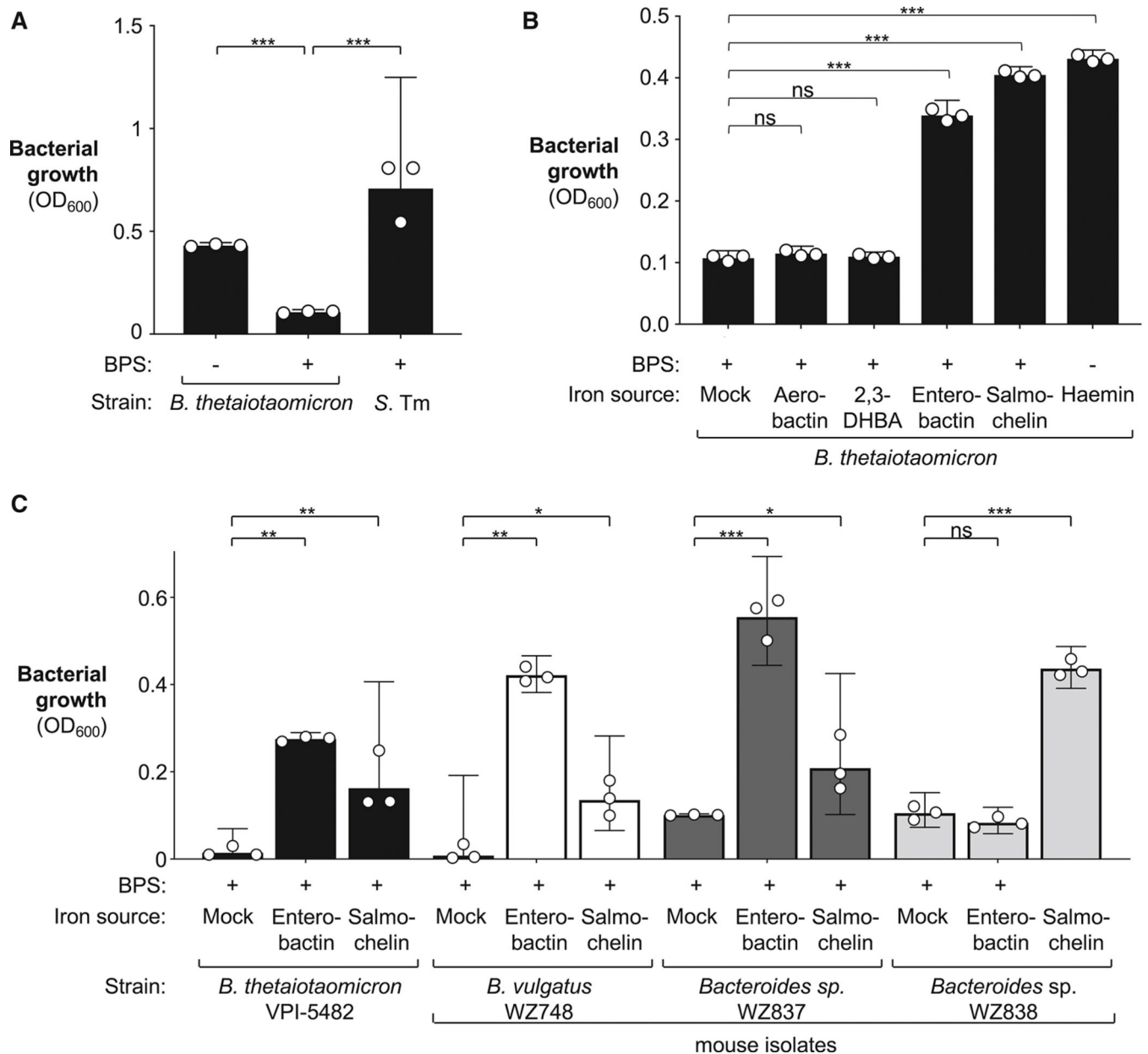
Figure 2: Utilization of enterobacterial siderophores by *Bacteroides* strains *in vitro*.
(**A**) *B. thetaiotaomicron* VPI-5482 Δ*tdk* or *S.* Tm SL1344 were anaerobically cultured in haemin-containing tryptone yeast extract glucose (TYG) medium in the presence or absence of 200 μmol/L of iron chelator bathophenanthroline disulfonate (BPS) for 36 hours. Bacterial growth was assessed by measuring optical density of the culture at a wavelength of 600 nm (OD_{600}). (**B** – **C**) *Bacteroides* strains were cultured in haemin-supplemented TYG medium before being subcultured in iron-limited (200 μmol/L of BPS) TYG medium supplemented with either 0.5 μM aerobactin, 0.5 μM 2,3-dihydroxybenzoic acid (2,3-DHBA), 0.5 μM enterobactin, or 2 μM salmochelin. Growth of *B. thetaiotaomicron* (**B**) and *Bacteroides* mouse isolates (**C**) was determined by measuring the optical density. See also

Fig. S1–3. Bars represent the geometric mean ± 95% confidence interval. *, $P < 0.05$; **, $P < 0.01$ ***, $P < 0.001$; ns, not statistically significant.
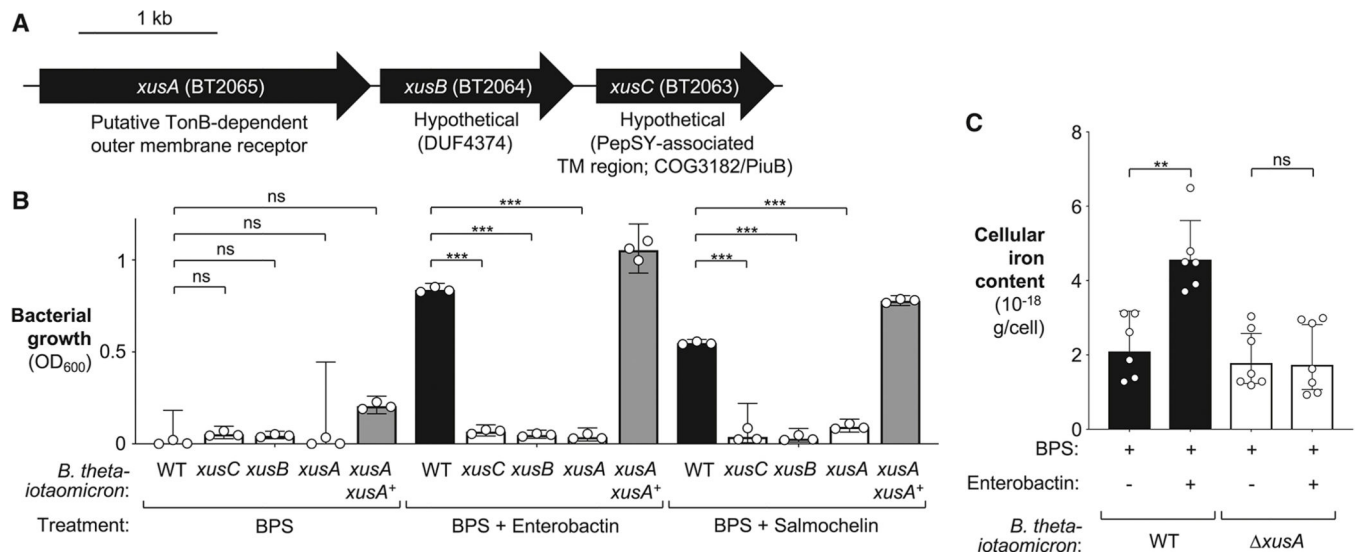
Figure 3: Role of the *B. thetaiotaomicron xusABC* operon in xenosiderophore uptake *in vitro*. (**A**). Schematic representation of the *xusABC* operon in *B. thetaiotaomicron* VPI-5482. (**B**) The indicated *B. thetaiotaomicron* strains were cultured in iron-limiting TYG medium supplemented with siderophores for 36 hours. The chelator bathophenanthroline disulfonate (BPS) was added at a concentration of 200 μmol/L. Enterobactin or salmochelin (50% iron saturation) were added at a final concentration of 0.5 μM and 2 μM, respectively. Growth was assessed by measuring optical density (OD_{600}). (**C**) The *B. thetaiotaomicron* wild-type strain and an isogenic *xusA* mutant were cultured in iron-deprived media to exhaust endogenous iron before being subcultured in the presence of iron-laden enterobactin or vehicle. Inductively Coupled Plasma Mass Spectrometry was used to assess cellular iron levels. Bars represent the geometric mean ± 95% confidence interval. **, $P < 0.01$ ***, $P < 0.001$; ns, not statistically significant.
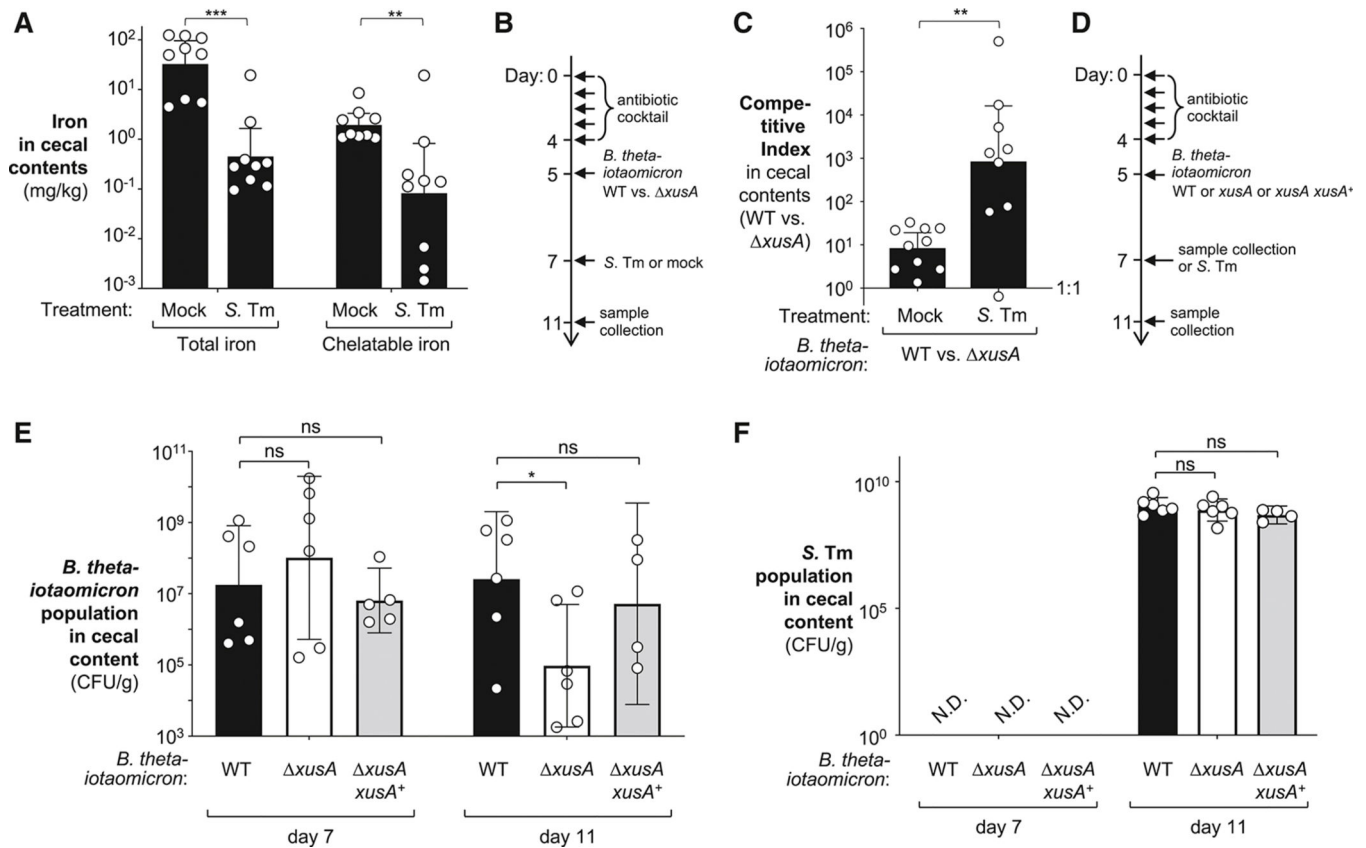
Figure 4: Role of *xusABC* locus in *B. thetaiotaomicron* colonization during murine *S*. Tm infection.

(**A**) Groups of streptomycin-treated C57BL/6 mice were either mock-treated (*N* = 9) or intragastrically inoculated with *S*. Tm SL1344 (*N* = 9). Four days after infection, the cecal contents were collected and separated into the chelatable and inaccessible iron fraction. The iron concentration was determined by ICP-MS. (**B – C**) Groups of C57BL/6 mice were treated with a cocktail of antibiotics, followed by intragastrical inoculation of an equal mixture of *B. thetaiotaomicron* wild-type strain (genomic signature tag 3; WZ433) and a *xusA* mutant (genomic signature tag 13; WZ647). Mice were mock-treated (LB, *N* = 10) or challenged with *S*. Tm SL1344 (*N* = 9) for 4 days. The abundance of each *B. thetaiotaomicron* strain in cecal contents was determined using qPCR targeting strain-specific signature tags. The competitive index was calculated as the ratio of the two strains in the cecal content, corrected by the ratio in the inoculum. A schematic representation of the experiment is shown in (**B**). Competitive index of *B. thetaiotaomicron* wild-type over *xusA* mutant in cecal contents (**C**). (**D – F**) Groups of C57BL/6 mice were treated with a cocktail of antibiotics, followed by intragastrical inoculation of either the *B. thetaiotaomicron* wild-type strain (*tdk*, Gen^R; *N* = 12), an isogenic *xusA* mutant (WZ777, Gen^R Cm^R, *N* = 12), or a complemented *xusA* mutant (WZ675, *xusA xusA*^+, *N* = 9). After two days, half of the animals in each group were euthanized to assess the colonization levels of these strains at homeostatic conditions, while the remaining groups were challenged with *S*. Tm SL1344 for 4 days. A schematic representation of the experiment is shown in (**D**). Abundance of indicated *B. thetaiotaomicron* (**E**) and *S*. Tm (**F**) strains in cecal contents as

determined by plating on selective agar. See also Fig. S4–6. Bars represent the geometric mean ± 95% confidence interval. *, $P < 0.05$; **, $P < 0.01$; ***; $P < 0.001$; ns, not statistically significant.
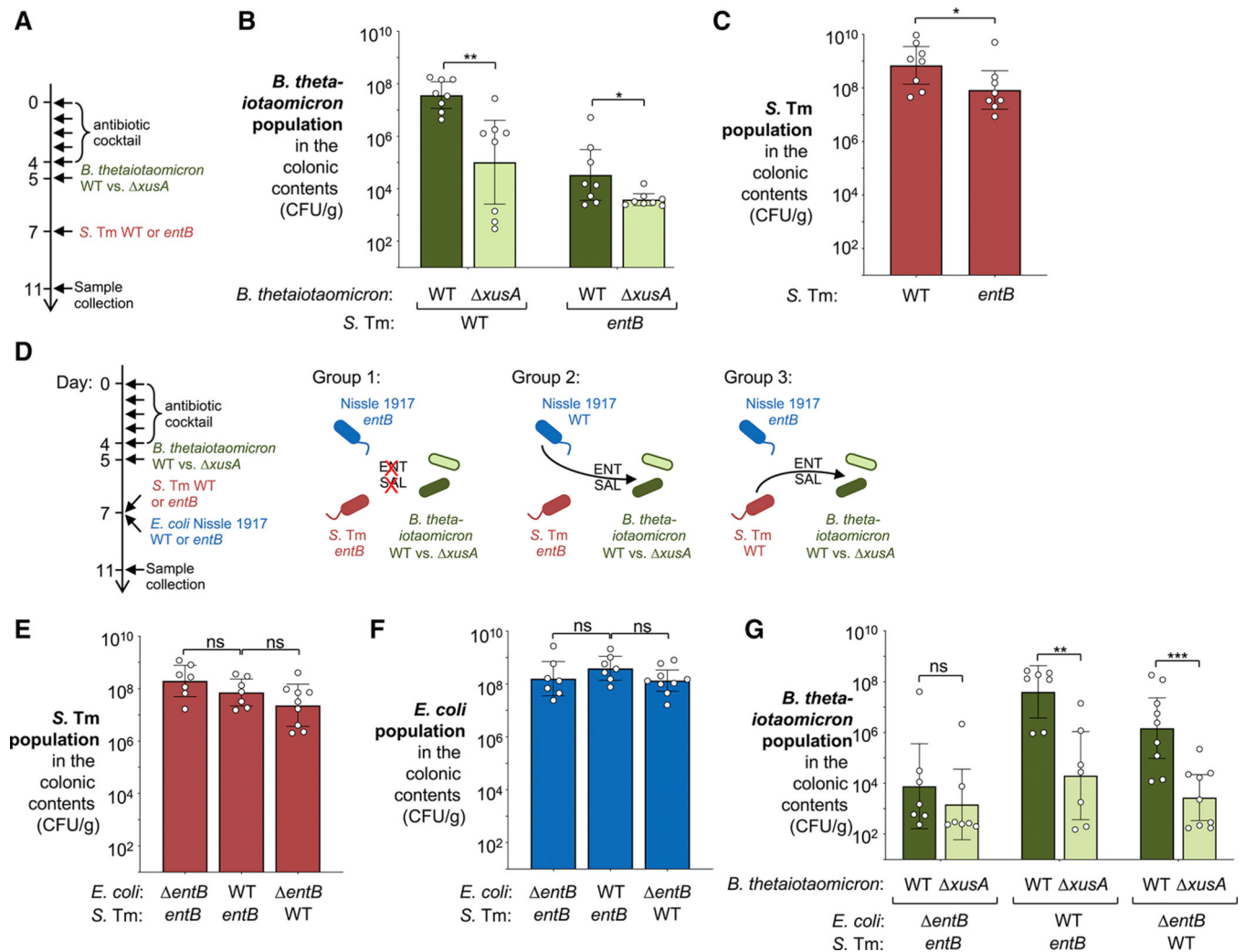
Figure 5: Contribution of enterobacterial siderophores to *B. thetaiotaomicron* fitness during infectious colitis.

(**A** – **C**) Groups of C57BL/6 mice were treated with a cocktail of antibiotics, followed by intragastrical inoculation of an equal mixture of the *B. thetaiotaomicron* wild-type strain (Δ*tdk*, Gen[R]) and a *xusA* mutant (WZ777, Gen[R] Cm[R]). Mice were then intragastrically inoculated with either *S*. Tm wild-type strain (SL1344; *N* = 8) or an *entB* mutant (WZ818; *N* = 8). (**A**) Schematic representation of the experiment. Four days after the *S*. Tm challenge, the abundance of *B. thetaiotaomicron* (**B**) and *S*. Tm (**C**) populations in the colonic contents was determined by plating on selective agar. (**D** – **G**) Groups of *Lcn2*^{−/−} mice were treated with a cocktail of antibiotics, followed by intragastrical inoculation of an equal mixture of the *B. thetaiotaomicron* wild-type strain (Δ*tdk*, Gen[R]) and a *xusA* mutant (WZ777, Gen[R] Cm[R]). Mice were then intragastrically inoculated with either an equal mixture of an *S*. Tm *entB* mutant (AR1258) and an *E. coli* Nissle 1917 *entB* mutant (WZ780) (*N* = 7, group 1), an equal mixture of an *S*. Tm *entB* mutant and the Nissle 1917 wild-type strain (WZ36) (*N* = 7, group 2), or an equal mixture of the *S*. Tm wild-type strain (IR715) and the Nissle 1917 *entB* mutant (WZ780) (*N* = 9, group 3). (**D**) Schematic representation of the experiment. Four days after the *S*. Tm challenge, the abundance of *S*. Tm (**E**), *E. coli* (**F**), and *B*.

thetaiotaomicron (**G**) populations in the colonic contents was determined by plating on selective agar. See also Fig. S4. Bars represent the geometric mean ± 95% confidence interval. *, $P < 0.05$; **, $P < 0.01$; ***; $P < 0.001$; ns, not statistically significant.
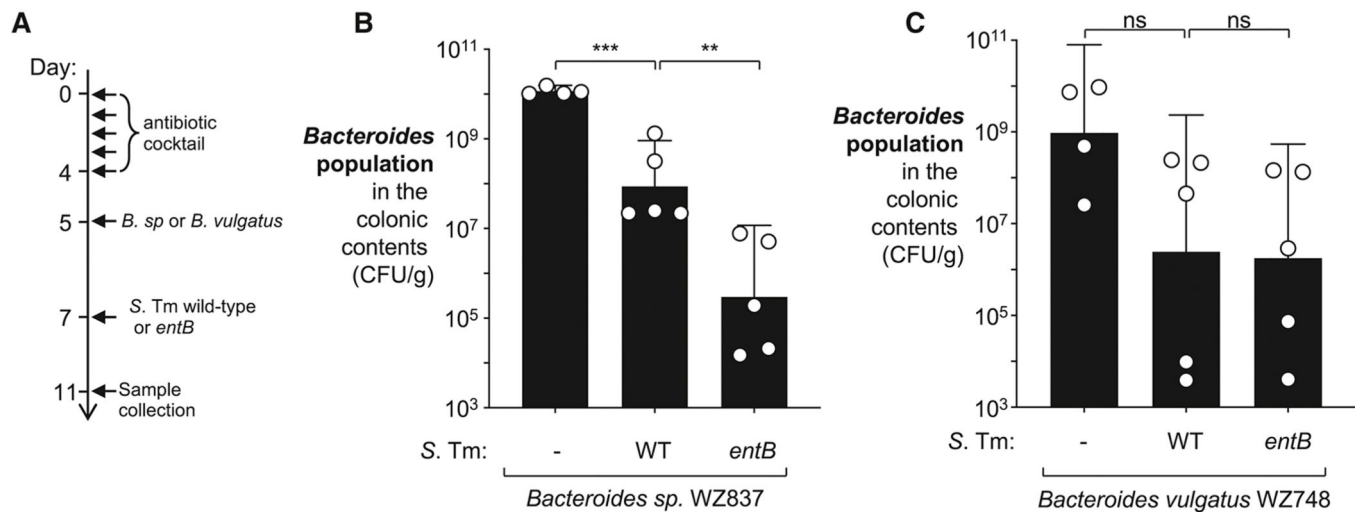
Figure 6: Contribution of siderophore utilization to fitness of *Bacteroides* isolates *in vivo*.
(**A – E**) Groups of C57BL/6 mice were treated with a cocktail of antibiotics, followed by intragastrical inoculation of *B. sp* (WZ837, Gen^R) or *B. vulgatus* (WZ748, Gen^R). Groups of mice either remained untreated (*N* = 4), or were intragastrically inoculated with the *S*. Tm wild-type strain (*N* = 5) or a *S*. Tm *entB* mutant (WZ818, *N* = 5). (**A**) Schematic representation of the experiment. Four days after the *S*. Tm inoculation, the abundance of *B. sp* (**B**) and *B. vulgatus* (**C**) populations in the colonic contents was determined by plating on selective agar. Bars represent the geometric mean ± 95% confidence interval. **, *P* < 0.01; ***, *P* < 0.001; ns, not statically significant.
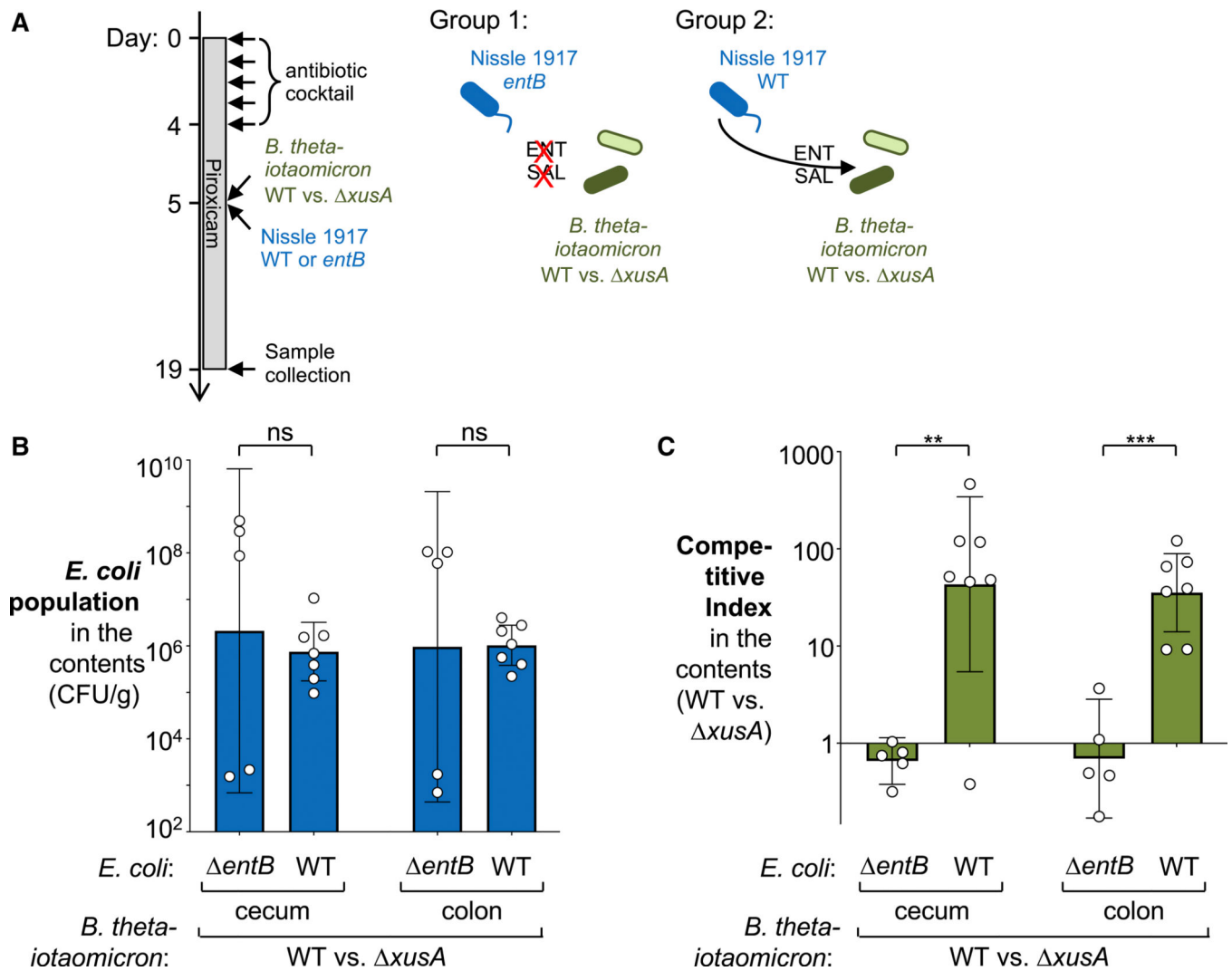
Figure 7: Contribution of Enterobacterial siderophores to *B. thetaiotaomicron* fitness during non-infectious colitis.

(**A** – **C**) Groups of *Il10⁻/⁻* mice were treated with a cocktail of antibiotics to allow stable engraftment of *B. thetaiotaomicron*. Piroxicam was administered in the mouse diet throughout the experiment. Mice were intragastrically inoculated with an equal mixture of *B. thetaiotaomicron* wild-type strain (*tdk*, Genᴿ) and a *xusA* mutant (WZ777, GenᴿCmᴿ), plus a Nissle 1917 *entB* mutant (WZ780) (*N* = 5, group 1) or the same *B. thetaiotaomicron* mixture plus the Nissle 1917 wild-type strain (WZ36) (*N* = 7, group 2). Fourteen days after bacterial inoculation, Nissle 1917 and *B. thetaiotaomicron* abundance in intestinal contents was determined by plating on selective agar. (**A**) Schematic representation of the experiment. (**B**) *E. coli* population in intestinal content. (**C**) Competitive index of *B. thetaiotaomicron* wild-type over *xusA* mutant in intestinal content. See also Fig. S7. Bars represent the geometric mean ± 95% confidence interval. **, *P* < 0.01 ***, *P* < 0.001; ns, not statistically significant.

KEY RESOURCES TABLE

REAGENT or RESOURCE	SOURCE	IDENTIFIER AND USAGE
Bacterial Strains		
Bacteroides thetaiotaomicron VPI-5482 *tdk* (Gen^R)	(Koropatkin et al., 2008)	VPI-5482
B. thetaiotaomicron *tdk* BT0159::Cm-cassette-signature-tag-3	This study	WZ433
B. thetaiotaomicron *tdk* BT0159::Cm-cassette-signature-tag-13	This study	WZ412
B. thetaiotaomicron *tdk* BT0159::Cm-cassette-signature-tag-15	This study	WZ413
B. thetaiotaomicron *tdk* BT0159::Cm-cassette-signature-tag-21	This study	WZ415
B. thetaiotaomicron *tdk* BT0159::Cm-cassette-signature-tag-24	This study	WZ418
B. thetaiotaomicron WZ412 BT_2063 (= *xusC*)	This study	WZ534
B. thetaiotaomicron WZ412 BT_2064 (= *xusB*)	This study	WZ697
B. thetaiotaomicron WZ412 BT_2065 (= *xusA*)	This study	WZ647
B. thetaiotaomicron WZ412 BT_2063-65	This study	WZ636
B. thetaiotaomicron WZ412 BT_0496	This study	WZ541
B. thetaiotaomicron WZ412 BT_2479	This study	WZ555
B. thetaiotaomicron WZ413 BT_2098-2100	This study	WZ553
B. thetaiotaomicron WZ413 BT_1950-1952	This study	WZ551
B. thetaiotaomicron WZ413 BT_2409	This study	WZ549
B. thetaiotaomicron WZ418 BT_0502-04	This study	WZ591
B. thetaiotaomicron WZ415 BT_1219	This study	WZ537
B. thetaiotaomicron WZ647 (BT_3743-3744)::BT_2065 (complemented)	This study	WZ675
B. thetaiotaomicron *tdk* BT_2065 (BT_3743-3744)::Cm^R	This study	WZ777
Bacteroides vulgatus (mouse isolate)	This study	WZ748
Bacteroides sp. (mouse isolate)	This study	WZ837
Bacteroides sp. (mouse isolate)	This study	WZ838
S. Tm wild-type strain (Nal^R)	(Stojiljkovic et al., 1995)	IR715
S. Tm wild-type strain (Strep^R)	(Hoiseth and Stocker, 1981)	SL1344
S. Tm IR715 *entB*::MudJ (Kan^R)	(Tsolis et al., 1995)	AR1258
S. Tm SL1344 *entB*::MudJ (Strep^R Kan^R)	This study	WZ818
S. Tm SL1344 *iroB* (Strep^R)	This study	WZ840
S. Tm SL1344 *iroN fepA cirA* (Strep^R)	This study	WZ692
Clostridium symbiosum	ATCC	ATCC 14940
E. coli wild-type strain (O6:K5:H1)	(Grozdanov et al., 2004)	Nissle 1917
E. coli Nissle 1917 (pWSK129) (Kan^R)	This study	WZ36
E. coli Nissle 1917 *entB*	This study	WZ532
E. coli Nissle 1917 *entB* (pWSK129) (Kan^R)	This study	WZ780
E. coli DH5α λ*pir*, F⁻ *endA1 hsdR17* (r⁻m⁺) *supE44 thi-1 recA1 gyrA relA1* (*lacZYA-argF*)*U189* φ*80lacZ* M15 λ*pir*	(Pal et al., 2005)	DH5α λ*pir*
E. coli S17-1 λ*pir*, *zxx::*RP4 2-(Tet^r::Mu) (Kan^r::Tn7) λ*pir*	(Simon et al., 1983)	S17-1 λ*pir*

REAGENT or RESOURCE	SOURCE	IDENTIFIER AND USAGE
Chemicals, Peptides, and Recombinant Proteins		
5-fluoro-2-deoxy-uridine	Ark Pharm	Cat#AK-24802
5,5′-[3-(2-Pyridyl)-1,2,4-triazine-5,6-diyl]difuran-2-sulfonic acid disodium salt	Sigma	Cat#P4272
Ammonium acetate	USB	Cat#11251
Agar	Thermo Fisher	Cat# BP1423
Ammonium Fe(III) citrate	Sigma	Cat# F5879
Ampicillin	Cayman Chemical Company	Cat# 14417
Bacteroides Bile Esculin Agar (BBE)	Becton Dickinson	Cat# 221836
Bathophenanthroline disulfonic acid disodium salt hydrate	Alfa Aesar	Cat# B23244
Brain-heart-infusion (BHI) media	Becton Dickinson	Cat# 237500
Bacto yeast extract	Becton Dickinson	#212750
$CaCl_2$ x 2 H_2O	Sigma	Cat#223506
Chelex 100 Resin	Biorad	Cat#142-1253
Chopped meat media	Remel	Cat# R05031
Chloramphenicol	Fisher Bioreagents	Cat#BP904-100
$CoCl_2$ x 6 H_2O	Sigma	Cat# 202185
$CuSO_4$	Sigma	Cat#C1297
L-Cysteine	Alfa Aesar	Cat#A10389
Defibrinated horse blood	Hemostat	Cat# DHB500
Difco LB agar-Miller	Becton Dickinson	Cat# 244520
Difco LB broth-Miller	Becton Dickinson	Cat# 244620
Dimethyl sulfoxide (DMSO)	Corning	Cat# MT-25950CQC
DNA-free DNA removal Kit	Invitrogen	Cat# AM1906
EDTA Disodium Salt	RPI	Cat# E57020-1000.0
Enterobactin, iron free	Sigma	Cat# E3910
$FeSO_4$	Sigma	Cat#F8633
Glucose	Fisher Chemical	Cat#D14-212
Hemin	Sigma	Cat#51280
Kanamycin	Fisher Chemical	Cat#BP906-5
KH_2PO_4	Fisher Chemical	Cat#P285
L-cysteine	Alfa Aesar	Cat#A10389
L-methionine	Sigma	Cat#M9625
Metronidazole	Sigma	Cat# M3761
$MgCl_2$ x 6 H_2O	Fisher Chemical	Cat#M33
$MgSO_4$ x 7 H_2O	Amresco	Cat#10034-99-8
$MnCl_2$ x 4 H_2O	Acros Organics	Cat#205891000
NaCl	RPI	Cat#S23020
$NaHCO_3$	Sigma	Cat#S6014

REAGENT or RESOURCE	SOURCE	IDENTIFIER AND USAGE
Nalidixic acid	Fisher Bioreagents	Cat#BP908-25
Neomycin trisulfate hydrate	Sigma	Cat# N1876
$(NH_4)_2SO_4$	Sigma	Cat#A4915
Nitric acid (TraceMetal™ Grade)	Fisher Chemicals	Cat# A509-P500
Nutrient broth base	Becton Dickinson	Cat# 234000
Menadione	Sigma	Cat#M9429
Protoporphyrin IX	Enzo Life Sciences	Cat# ALX-430-041-G001
Peptone	Becton Dickinson	Cat#211684
Resazurin	Sigma	Cat#R7017
Salmochelin S4, iron free	EMC Microcollections	Cat# SAL-S4
Sodium molybdate dihydrate	Sigma	Cat#M-1003
Streptomycin sulfate	VWR	Cat# 97061-528
Sucrose	Fisher Science Education	Cat#S25590B
SYBR Green qPCR Master Mix	Life Technologies	Cat# 4309155
TaqMan reverse transcription reagents	Invitrogen	Cat# N8080234
Thioglycollate media	Sigma	Cat# 90404
TRI reagent	Molecular research center	Cat# TR118
Tryptone	Thermo Fisher	Cat#BP1421
Vancomycin	Chem-Impex INT'L INC	Cat# 00315
Vitamin B_{12}	Sigma	V2876
Lysing Matrix B	MP Biomedicals	Cat# 6911050
Zinc chloride	Sigma	Cat#208086
Critical Commercial Assays		
QIAamp PowerFecal DNA Isolation Kit	Qiagen	Cat# 12830-50
RNeasy PowerMicrobiome Kit	Qiagen	Cat# 26000-50
TruSeq Stranded Total RNA Library Prep Kit	Illumina	Cat# 20020598
RNAlater™ Stabilization Solution	Thermo Fisher	Cat# AM7020
TOPO cloning kit	Invitrogen	Cat# K457502
Gibson Assembly Cloning Kit	NEB	Cat# E2611
Q5 Hot Start 2x Master Mix	NEB	Cat# M0494L
DNA-free™ DNA Removal Kit	Invitrogen	Cat#AM1906
Deposited Data		
RNA-seq data	European Nucleotide Archive	PRJEB33026
Experimental Models: Organisms/Strains		
SPF C57BL/6 mice (wild-type)	The Jackson Laboratory	Cat# 000664
SPF B6.129P2-$Il10^{tm1Cgn}$/J ($Il10^{-/-}$)	The Jackson Laboratory	Cat# 002251
SPF B6.129P2-$Lcn2^{tm1Aade}$/AkiJ ($Lcn2^{-/-}$)	The Jackson Laboratory	Cat# 024630
Wild-type Swiss Webster (ex-germ-free)	(Spiga et al., 2017)	N/A

REAGENT or RESOURCE	SOURCE	IDENTIFIER AND USAGE
Recombinant DNA		
pKNOCK-*bla-ermGb*::*tdk*	(Koropatkin et al., 2008)	pExchange-*tdk*
pExchange-*tdk*::intergenic region of BT_3743 and BT_3744	This study	pKI
ori(*R6K*) *mobRP4 sacRB* Kan^R	(Hughes et al., 2017)	pGP706
ori(pSC101) *lacZα* Kan^R	(Wang and Kushner, 1991)	pWSK129
pExchange-*tdk*:: BT_0159:: BT0159::Cm-cassette-signature-tag-3	This study	pWZ433
pExchange-*tdk*:: BT_0159:: BT0159::Cm-cassette-signature-tag-13	This study	pWZ412
pExchange-*tdk*:: BT_0159:: BT0159::Cm-cassette-signature-tag-15	This study	pWZ413
pExchange-*tdk*:: BT_0159:: BT0159::Cm-cassette-signature-tag-21	This study	pWZ415
pExchange-*tdk*:: BT_0159:: BT0159::Cm-cassette-signature-tag-24	This study	pWZ418
Upstream and downstream regions of *E. coli* Nissle 1917 *entB* in pGP706	This study	pWZ517
Upstream and downstream regions of *B. theta BT_2063* in pExchange-tdk	This study	pWZ498
Upstream and downstream regions of *B. theta BT_2065* in pExchange-tdk	This study	pWZ628
Upstream and downstream regions of *B. theta BT_2063-65* in pExchange-tdk	This study	pWZ630
Upstream and downstream regions of *B. theta BT_0496* in pExchange-tdk	This study	pWZ496
Upstream and downstream regions of *B. theta BT_2479* in pExchange-tdk	This study	pWZ500
Upstream and downstream regions of *B. theta BT_2098-2100* in pExchange-tdk	This study	pWZ502
Upstream and downstream regions of *B. theta BT_1950-52* in pExchange-tdk	This study	pWZ504
Upstream and downstream regions of *B. theta BT_2409* in pExchange-tdk	This study	pWZ506
Upstream and downstream regions of *B. theta BT_0502-04* in pExchange-tdk	This study	pWZ508
Upstream and downstream regions of *B. theta BT_1219* in pExchange-tdk	This study	pWZ510
Upstream and downstream regions of *S.*Tm *iroN* in pGP706	This study	pWZ626
Upstream and downstream regions of *S.*Tm *fepA* in pGP706	This study	WZ650
Upstream and downstream regions of *S.*Tm *cirA* in pGP706	This study	pWZ681
Upstream and downstream regions of *S.*Tm *iroB* in pGP706	This study	pWZ842
Promoter and open reading frame of *B. theta BT_2065* in pKI	This study	pWZ661
16S rDNA fragment of *E. coli* K-12 cloned into pCR2.1	(Winter et al., 2013)	pSW196
16S rDNA fragment of a member of the order Clostridiales cloned into pCR2.1	(Bacchetti De Gregoris et al., 2011; Winter et al., 2013)	pSW325
16S rDNA fragment of a Coriobacteriaceae family member cloned into pCR2.1	(Bacchetti De Gregoris et al., 2011; Winter et al., 2013)	pSW326
Software and Algorithms		
Excel for Mac 2016	Microsoft	N/A
Prism V8.1.1.	Graph Pad	https://www.graphpad.com/scientific-software/prism/
DESeq2 V1.22.2	(Love et al., 2014)	http://bioconductor.org/packages/release/bioc/html/DESeq2.html
BBMap V36.20	DOE Joint Genome Institute	https://github.com/BioInfoTools/BBMap/releases/tag/v36.20

REAGENT or RESOURCE	SOURCE	IDENTIFIER AND USAGE
featureCounts V1.5.1	(Liao et al., 2014)	http://subread.sourceforge.net/
Bowtie2 V2. 29	(Langmead and Salzberg, 2012)	http://bowtie-bio.sourceforge.net/bowtie2/index.shtml
MacVector V13.5.2	MacVector	https://macvector.com/downloads.html
Oligonucleotides		
Information regarding oligonucleotides used in this study is listed in Table S2.		